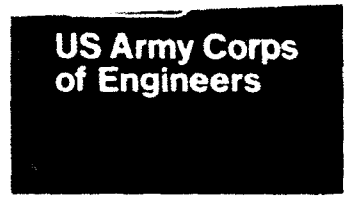

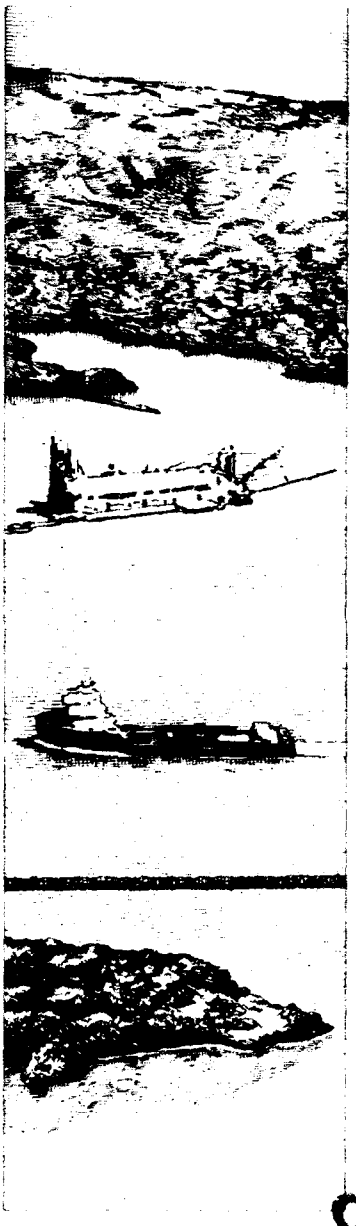

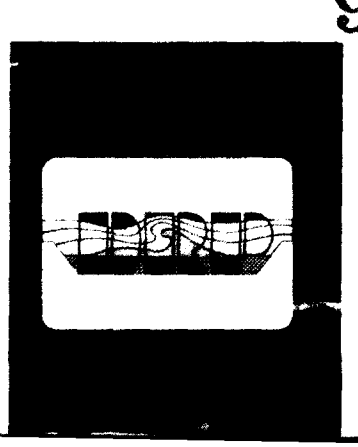

DREDGING RESEARCH PROGRAM

TECHNICAL REPORT DRP-92-3

BOUNDARY STRESSES AND VELOCITY PROFILES IN ESTUARINE FLOWS

Report 1
INTERIM CALCULATION METHODS

by

William H. McAnally, Jr., Earl J. Hayter

Hydraulics Laboratory

DEPARTMENT OF THE ARMY
Waterways Experiment Station, Corps of Engineers
3909 Halls Ferry Road, Vicksburg, Mississippi 39180-6199

August 1992

Report 1 of a Series

Prepared for DEPARTMENT OF THE ARMY
US Army Corps of Engineers
Washington, DC 20314-1000

Monitored by Coastal Engineering Research Center
US Army Engineer Waterways Experiment Station
3909 Halls Ferry Road, Vicksburg, Mississippi 39180-6199

Under Work Unit No. 32590

The Dredging Research Program (DRP) is a seven-year program of the US Army Corps of Engineers. DRP research is managed in these five technical areas:

Area 1 - Analysis of Dredged Material Placed in Open Water

Area 2 - Material Properties Related to Navigation and Dredging

Area 3 - Dredge Plant Equipment and Systems Processes

Area 4 - Vessel Positioning, Survey Controls, and Dredge Monitoring Systems

Area 5 - Management of Dredging Projects

US Army Corps
of Engineers
Waterways Experiment
Station

Dredging Research Program Report Summary

Boundary Stresses and Velocity Profiles in Estuarine Flows; Report 1, Interim Calculation Methods

ISSUE: Corps dredging operation elements must often assess the retention of material at dredged material disposal sites to determine site capacity for future dredging work. This is routinely done by bathymetric surveys of the site. In some cases, predictions must be made of sediment erosion processes that might occur at the site under certain assumed conditions, such as for a different sediment type. Erosion depends strongly on bed shear stress. A variety of approaches are available to calculate boundary layer properties such as shear stress. The issue is to determine which method is most appropriate when conditions are complicated by tidal influences.

RESEARCH: The Dredging Research Program (DRP) includes guidance and procedures for predicting movements of dredged material placed in open water. An important part of DRP research is to check predictive techniques against data, as was done here.

SUMMARY: Conditions that can be encountered in estuarine areas include tidally reversing flows, density stratification, suspended sediment contributions, and combined current and wind-wave effects. Possible approaches to making boundary layer calculations include modified steady-flow equations, variable eddy viscosity and mixing length equations, and turbulence transport equations. Interim recommendations for calculation methods are based on the situation and the computational power available.

AVAILABILITY OF REPORT: The report is available through the Interlibrary Loan Service from the US Army Engineer Waterways Experiment Station (WES) Library, telephone number (601) 634-2355. National Technical Information Service (NTIS) report numbers may be requested from WES Librarians.

To purchase a copy of the report, call NTIS at (703) 487-4780.

About the Authors: Mr. William H. McAnally, Jr., is the Chief of the Estuaries Division, Hydraulics Laboratory, U.S. Army Engineer Waterways Experiment Station. Dr. Earl J. Hayter is an Associate Professor in the Department of Civil Engineering at Clemson University, Clemson, South Carolina. Dr. Hayter was under the Intergovernmental Personnel Act agreement during the time of this study. For further information about the DRP, contact Mr. E. Clark McNair, Jr., Manager, DRP, at (601) 634-2070.

August 1992

REPORT DOCUMENTATION PAGE

Form Approved
OMB No 0704-0188

1. AGENCY USE ONLY (Leave blank)	2. REPORT DATE	3. REPORT TYPE AND DATES COVERED
	August 1992	Report 1 of a series

4. TITLE AND SUBTITLE

Boundary Stresses and Velocity Profiles in Estuarine Flows; Interim Calculation Methods

5. FUNDING NUMBERS

WU 32590

6. AUTHOR(S)

William H. McAnally, Jr.
Earl J. Hayter

7. PERFORMING ORGANIZATION NAME(S) AND ADDRESS(ES)

USAE Waterways Experiment Station, Hydraulics Laboratory, 3909 Halls Ferry Road, Vicksburg, MS 39180-6199

8. PERFORMING ORGANIZATION REPORT NUMBER

9. SPONSORING/MONITORING AGENCY NAME(S) AND ADDRESS(ES)

Department of the Army, US Army Corps of Engineers, Washington, DC 20314-1000

USAE Waterways Experiment Station, Coastal Engineering Research Center, 3909 Halls Ferry Road, Vicksburg, MS 39180-6199

10. SPONSORING/MONITORING AGENCY REPORT NUMBER

Technical Report DRP-92-3

11. SUPPLEMENTARY NOTES

Available from National Technical Information Service, 5285 Port Royal Road, Springfield, VA 22161.

12a. DISTRIBUTION/AVAILABILITY STATEMENT

Approved for public release; distribution is unlimited.

12b. DISTRIBUTION CODE

13. ABSTRACT (Maximum 200 words)

Calculation of sediment entrainment and transport rates at open water dredged material placement sites in tidal waters requires accurate descriptions of velocity profiles and stresses on the sediment bed. Standard equations for calculations in steady, uniform flows can give misleading results when applied in tidal waters. Complicating factors in tidal water environments include tidally reversing flows, density stratification, suspended sediment contributions, and combined current and wind-wave effects. Possible approaches to making calculations in this environment include (a) modified applications of the steady-flow equations, (b) time- and space-varying eddy viscosity and mixing length equations, and (c) turbulence transport equations. Interim recommendations for calculation methods are based on the situation and the computational power available.

14. SUBJECT TERMS

Boundary layers
Estuaries
Stresses
Turbulence closure
Velocity profiles

15. NUMBER OF PAGES

92

16. PRICE CODE

17. SECURITY CLASSIFICATION OF REPORT	18. SECURITY CLASSIFICATION OF THIS PAGE	19. SECURITY CLASSIFICATION OF ABSTRACT	20. LIMITATION OF ABSTRACT
UNCLASSIFIED	UNCLASSIFIED		

PREFACE

This study was conducted at the Hydraulics Laboratory (HL) for the Coastal Engineering Research Center (CERC), US Army Engineer Waterways Experiment Station (WES). The work described herein was authorized as part of the Dredging Research Program (DRP) of the Headquarters, US Army Corps of Engineers (HQUSACE), and was performed under Work Unit 32590, "Calculation of Boundary Layer Properties (Cohesive Sediments)." Messrs. Glenn R. Drummond, Rixie J. Hardy, Vincent Montante, and John J. Parez are DRP Technical Monitors from HQUSACE. Mr. E. Clark McNair, Jr., CERC, is Program Manager (PM) for the DRP, and Dr. Lyndell Z. Hales, CERC, is Assistant PM. Dr. Nicholas C. Kraus, Senior Scientist, CERC, is the Manager for DRP Technical Area 1, Analysis of Dredged Material Placed in Open Waters.

This study was performed and the report prepared over the period 1 October 1988 through 30 September 1989 by Mr. William H. McAnally, Jr., Chief, Estuaries Division (ED), HL, and Dr. Earl J. Hayter, Clemson University, Clemson, SC, who conducted his research under the Intergovernmental Personnel Act under the general supervision of Messrs. Frank A. Herrmann, Jr., Director, HL, and Richard A. Sager, Assistant Director, HL. Mr. Allen M. Teeter, ED, was Principal Investigator of Work Unit 32590. Dr. Kraus reviewed the report. Mrs. Marsha C. Gay, Information Technology Laboratory, WES, edited the final report.

At the time of publication of this report, Director of WES was Dr. Robert W. Whalin. Commander was COL Leonard G. Hassell, EN.

For further information on this report or on the Dredging Research Program, please contact Mr. E. Clark McNair, Program Manager, at (601) 634-2070.

FOREWORD

In 1932 Sir Horace Lamb said, "I am an old man now, and when I die and go to heaven there are two matters on which I hope for enlightenment. One is quantum electrodynamics, and the other is turbulent motion of fluids. About the former I am really rather optimistic."* Fifty-eight years later, we have little more reason for optimism than did Sir Horace. We have made progress in the sense that there are several more options for mathematically describing fluid turbulence and its offspring, fluid stresses; however, these options are less the result of improved physical understanding than of hugely increased computational capabilities.

We share Sir Horace's hope for enlightenment, but confess that the techniques recommended here do not provide that enlightenment. They simply provide means of computing stresses that are the best currently available engineering approximations.

---

* R. J. Donnelly. 1988 (Nov). "Superfluid Turbulence," Scientific American, p 100.

CONTENTS

CONVERSION FACTORS, NON-SI TO SI (METRIC)
UNITS OF MEASUREMENT

Non-SI units of measurement used in this report can be converted to SI (metric) units as follows:

Multiply	By	To Obtain
cubic feet	0.02831685	cubic metres
degrees (angle)	0.01745329	radians
feet	0.3048	metres

SUMMARY

Calculation of sediment entrainment and transport rates at open water dredged material placement sites in tidal waters requires accurate descriptions of velocity profiles and stresses on the sediment bed. Standard equations for calculations in steady, uniform flows can give misleading results when applied in tidal waters. For example, standard log profiles adapted from steady-flow equations can generate bed shear stress values that are wrong by a factor of two or more and are in the wrong direction as well.

Complicating factors in tidal water environments include tidally reversing flows in which accelerations and decelerations strongly affect the velocity profile and bed shear. Density stratification, common in estuaries, can likewise generate profiles that drastically differ from those seen in homogeneous flows. Suspended sediment contributions and deformable mud beds also interact with the flow, altering the stresses experienced by sediment beds. Combined current and wind wave effects lead to stresses on the bed that are not simply linear combinations of their individual effects.

Possible approaches to making calculations in this environment include (a) modified applications of the steady-flow equations, (b) time- and space-varying eddy viscosity and mixing length equations, and (c) turbulence transport equations.

Interim recommendations for calculation methods are based on the situation and the computational power available:

a. For simple calculations, equations using a spatially variable eddy viscosity are recommended. Where density stratification and/or sediment suspension conditions are significant, modifications to the eddy viscosity equations are justified. Different sets of equations are recommended for tidal currents alone and for tidal currents with short-period waves present.

b. For three-dimensional numerical modeling, a turbulence transport model using a two-equation closure is recommended.

Laboratory and field tests are needed to confirm these recommendations and to extend them to more realistic environmental conditions.

BOUNDARY STRESSES AND VELOCITY PROFILES IN ESTUARINE FLOWS

INTERIM CALCULATION METHODS

PART I: INTRODUCTION

Objectives

1. The primary objective of this work is to provide improved descriptions of boundary layer velocity profiles and stresses in estuarine flows such that more accurate and reliable computations can be made for dredged material erosion and transport. The purpose of this report is to establish the best methods currently available to calculate estuarine velocity profiles and stresses. A subsequent report will provide updated recommendations.

Background

2. Accurate computation of sediment deposition, erosion, entrainment, and transport requires realistic calculation of near-bed flows and effective stresses. Deposition and erosion rate expressions for cohesive sediments typical of estuaries include the effective shear stress exerted on the bed as a basic variable. The near-bed velocity profile and turbulent exchanges control the rate of transport of sediments traveling close to the bed.

3. While this important subject has been thoroughly explored for steady, constant-density flows, it has been largely neglected for estuarine flows, which are typically unsteady (due to astronomical and wind tides, surges, and short-period waves), nonuniform, and variable density (due to freshwater-saltwater interaction plus temperature and suspended sediment). Near-bed processes for short-period waves have been examined somewhat more fully because of the obvious inadequacies of traditional approaches, but the mathematical descriptions of those are still inadequate to use in computations involving estuaries. Estuarine flows have usually been described using the traditional steady-flow methods without modification, despite the fact that they can give erroneous or even nonsensical results.

4. As part of an earlier attempt to develop computational procedures for a two-dimensional numerical model of sediment transport, some ad hoc

solutions to this problem were developed (Thomas and McAnally 1985). The work described here is an attempt to improve upon that approach and set a framework for future significant improvements.

Character of Estuarine Flows and Boundary Stresses

5. Two aspects of estuaries require a method of evaluation of estuarine currents different from the usual steady, uniform case. First, their oscillatory nature creates time-dependent accelerations that alter the thickness and velocity profile of the bottom boundary layer. Second, freshwater runoff meeting saline ocean water creates longitudinal, and usually lateral and vertical, density gradients that cause the ambient vertical velocity profile to be substantially different from the classic forms. Figure 1 illustrates the general nature of the vertical and longitudinal structures of estuarine flows.

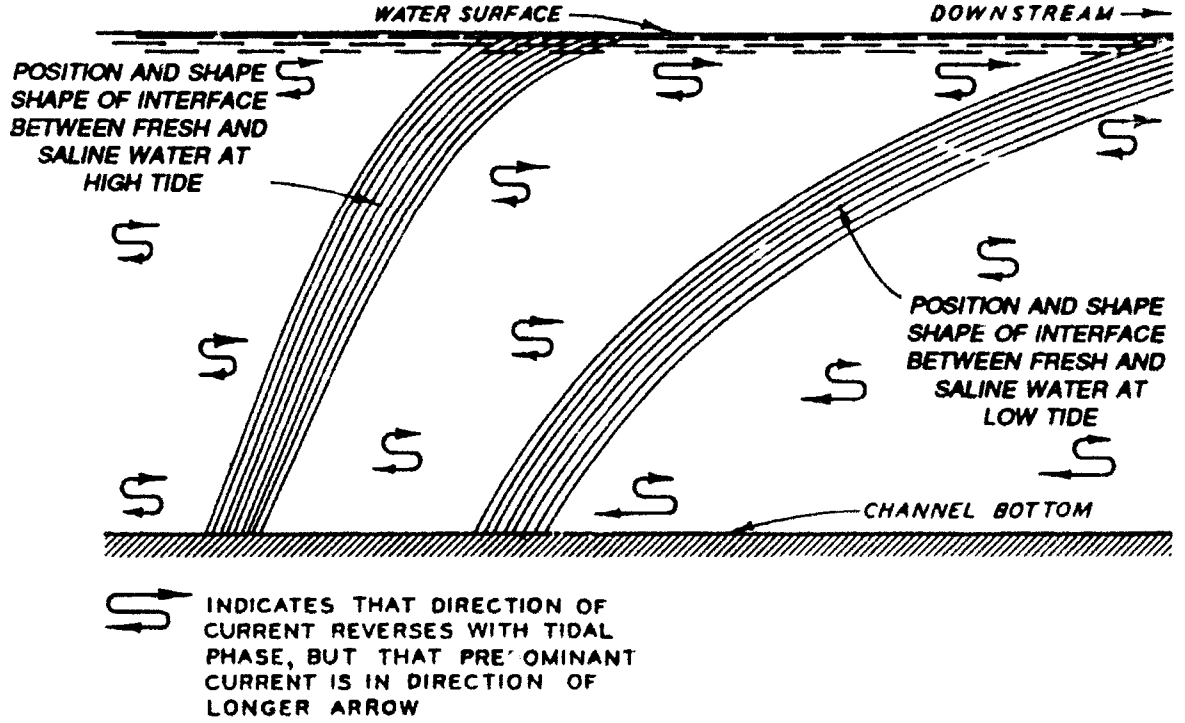

Figure 1. Schematic vertical and longitudinal current structure of estuarine flows

6. Unlike unidirectional flows, in which the entire depth of flow may be occupied by the boundary layer, estuarine boundary layers grow between successive slack-water periods; thus, their thickness may be small with respect to the water depth during a significant portion of the tidal cycle. This has

significant implications with regard to use of standard velocity profile equations and constant coefficients for computing stresses. Several researchers have observed that shear stresses are dependent on the pressure gradient as well as the flow speed. Gordon (1975) measured Reynolds stresses in a tidal current and concluded that bed shear stresses were considerably larger during decelerating flows, i.e., when the pressure gradient was in opposition to the direction of the current, than during accelerating flows.

Soft Sediment Boundaries

7. The bed elevation in open channels is usually defined as the location at which the flow velocity is zero. Where beds are rigid, this definition is appropriate; but for mobile sand beds the definition lacks precision and for soft muds it may be substantially erroneous.

8. In many estuarine situations, sediment concentration and bulk density increase rapidly near the bed, and often do so without a clearly defined interface between water and mud. In the words of W. R. Parker (Blackdown Consultants, Taunton, England), as the bed is approached, the suspension changes gradually "from muddy water to watery mud to bed" without a definite interface. Under these conditions, defining the bed elevation becomes a matter of selecting an arbitrary definition, usually based on density.

9. A density-defined bed interface need not correspond to the zero velocity location, since at any given moment the high-density suspension may flow to a significant depth or it may possess sufficient structure (stationary suspension) to hold it apparently motionless. In either case, ordinary definitions of the boundary and boundary layer are often inappropriate.

Scope

10. This work is intended to be limited to conditions characteristic of placement of dredged material in estuarine sites in the United States, though the applicability may be wider than that. The emphasis is on sites where the transport mechanisms are primarily currents with some contribution by non-breaking waves. A parallel investigation on wave-dominated environments is reported separately (Madsen and Wikramanayake 1988). This report is concerned with existing theory and experiments and how they may be best adapted to

engineering calculations for sediment transport at open-water dredged material placement sites. Sediment transport calculations will be dealt with separately.

PART II: HYDRODYNAMIC AND BOUNDARY LAYER FUNDAMENTALS

Basic Equations

11. Present hydrodynamic analyses almost universally begin with the Eulerian view Navier-Stokes equations for conservation of mass and momentum in free surface flows, which, expressed in tensor notation, are

$$\frac{D\hat{\rho}}{Dx_i} = \frac{\partial \hat{\rho}}{\partial t} + \frac{(\partial \hat{\rho} \hat{u}_i)}{\partial x_i} = 0 \tag{1}$$

$$\frac{D(\hat{\rho}\hat{u}_i)}{Dt} = - \frac{\partial \hat{P}}{\partial x_i} - \hat{\rho} g_i + \frac{\partial \hat{\tau}_{ij}}{\partial x_j} \tag{2}$$

where*

ρ = fluid density

x = spatial coordinate

t = time

u = flow velocity

P = pressure

g = acceleration due to gravity

τ = bed shear stress

i,j,k = coordinate axis designator, 1, 2, or 3 with repeated index summation

$\hat{}$ = indicates instantaneous value

An equation for conservation of constituents in transport is added

$$\rho \frac{D\hat{\theta}_n}{Dt} = \frac{\partial}{\partial x_i} \left(E_D \hat{\theta}_n \right) + \phi_n \tag{3}$$

---

* For convenience, symbols and unusual abbreviations are listed and defined in the Notation (Appendix A). The notation for Parts II and III is listed separately from that for Part IV, as symbols may have different meanings for the different areas of study covered in each Part.

where

θ = concentration of constituent

n = subscript indicating the constituent (e.g. salinity, temperature, or sediment)

E_D = Fickian diffusion coefficient

ϕ = sum of sinks and sources for θ

An equation of state completes the set of equations:

$$\hat{\rho} = f(\hat{\theta}_n) \tag{4}$$

For turbulent flows in large bodies of water, the instantaneous variables of Equations 1-4 are replaced with a summation of a time-mean value (averaged on the order of minutes) and an instantaneous fluctuation about that mean; for example,

$$\hat{u} = u + u' \tag{5}$$

where the prime indicates a quantity fluctuating in time. Replacement of the instantaneous values with the form of Equation 5 and performing algebraic manipulation results in a number of additional terms. Performing a second time-averaging step (which causes some terms to become equal to zero), neglecting some terms that make apparently minor contributions (including spatial variations in density except in the pressure term), and adding a term for the Coriolis effect results in

$$\frac{D\rho}{Dt} = \frac{\partial \rho}{\partial t} + \frac{\partial}{\partial x_i}(\rho u_i) = 0 \tag{6a}$$

$$\rho \frac{Du_i}{Dt} = -\frac{\partial P}{\partial x_i} - \rho g_i - \rho e_{ijk}\Omega_j u_k + \frac{\partial}{\partial x_j}\left(\overline{-\rho u_j' u_i'}\right) \tag{6b}$$

$$\rho \frac{D\theta_n}{Dt} = \frac{\partial}{\partial x_i}\left(\overline{-\rho u_j' \theta_n'}\right) + \phi_n \tag{6c}$$

$$\rho = f(\theta_n)$$

where

e = alternating tensor

Ω = Coriolis effect parameter

n = index for multiple constituents in transport

12. The overbar terms in equation set 6 are time averages of the products of fluctuating variables and are described as Reynolds stresses (Equation 6b) or Reynolds fluxes (Equation 6c). Defining these terms becomes the turbulence closure, which is a fundamental problem in practical use of the equations. That problem is discussed in Part III of this report.

Laminar and Turbulent Flows

13. Flows of interest here are usually fully turbulent in terms of the overall Reynolds number criterion. Boundary layers are not necessarily fully turbulent, though. The boundary Reynolds number of Nikuradse has been adopted by marine researchers, including Sternberg (1968), who defined the turbulence characteristics as follows:

a. Smooth turbulent when $R_p < 5.5$

b. Transitional when $5.5 < R_p < 165$

c. Rough turbulent when $165 < R_p$

where

$$R_p = \frac{u_* k_s}{\nu} \tag{7}$$

and

u_* = shear velocity

k_s = roughness element size

ν = kinematic viscosity

Boundary Layer Structure

14. Boundary layers in open channel flow are the zones near the boundary where drag exerted by the bed has a pronounced effect on the flow. The boundary layer is characterized by steep velocity gradients normal to the bed

and a corresponding increase in turbulent and viscous stresses.

15. The boundary layer thickness can be defined in several ways. In steady viscous flow it is commonly defined as the point at which the velocity reaches 99 percent of the free stream velocity or a similar measure in terms of the inviscid flow condition. While none of these definitions is particularly precise, they are useful in describing the flow profiles and bed stresses.

16. Turbulent boundary layers exhibit zones in which properties of the flow differ. Figure 2 illustrates zone subdivisions. Figure 2a shows a prevalent subdivision of steady-flow boundary layers. The size and existence of the viscous (laminar) sublayer and buffer zone are affected by the degree of turbulence and texture of the boundary, and, for fully rough turbulent flow, they may disappear.

17. For smooth turbulent flows, the viscous sublayer thickness is much greater than k_s , while for transitional and rough turbulent flows it is approximately equal to and much less than k_s , respectively. Thus as turbulence increases, bottom roughness plays an increasing role in the nature of the boundary layer.

18. Figure 2b shows the structure terminology used by Soulsby (1983) for marine boundary layers. The bed layer can be either laminar (when the bed is sufficiently smooth) or turbulent. Soulsby refers to the second zone as the log layer, where classical profile equations are thought to apply, and to the third zone as the outer layer. In the outer layer, structure depends on the free streamflow behavior, and thus the classical equations do not apply. Above the outer layer is the free stream zone, where velocity profile is essentially unaffected by the bed.

19. The boundary layer structure in estuarine flows is in general significantly altered by the presence of both tidal currents and wind-generated surface waves. The superposed current and high-frequency oscillatory water particle motion beneath a water wave interact in a nonlinear manner and result in a change in both the magnitude and direction of the bed stresses. For combined wave and current flows, a wave boundary layer develops in the zone immediately above the bottom. The thickness of this boundary layer is given by $\kappa u_{*cw}/\sigma$, where κ is von Karman's turbulence constant, σ is wave frequency, and u_{*cw} is wave- and current-induced shear velocity. Within the wave boundary layer, turbulence production is due to both wave and current

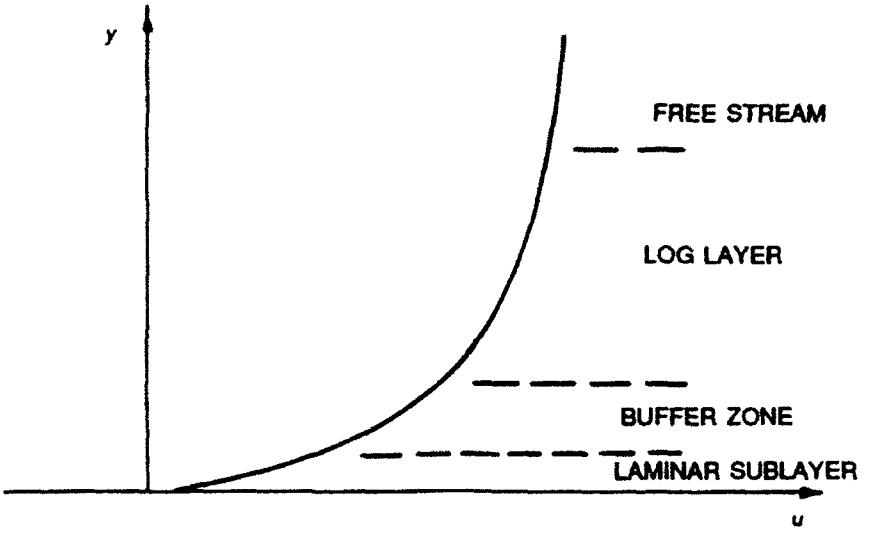

a. Typical subdivision of steady-flow boundary layers

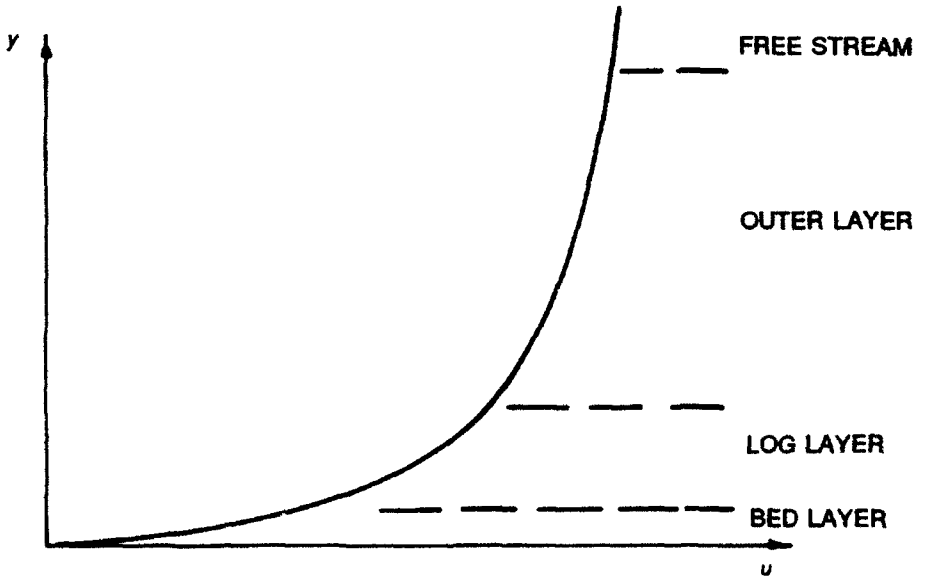

b. Soulsby (1983) subdivision of marine boundary layers

Figure 2. Boundary layer subdivisions

motion. A large-scale rotating current boundary layer extends from the bottom to the free stream zone (when the latter is present) or the water surface. In the portion of the current boundary layer that extends above the wave boundary layer, turbulence is associated with the oscillatory tidal current only.

Boundary Stresses

20. Stresses experienced by the sediment bed are complex products of the interaction of flow and bed. For convenience, these stresses are commonly divided into tangential and normal stresses. Many analyses divide them into surface and form stresses. Surface stress (or drag) is that which would occur if the bed were plane, and it can be described in terms of the height by which sediment grains protrude into the flow. Form stress is that caused by irregularities in the boundary, such as ripples or dunes.

21. Bed stresses contributing to sediment transport are often conceived of and described as tangential, even when they contain normal components (as in form drag). In some analyses, the normal lift force is assumed to be proportional to the tangential shear stress and thus is included implicitly. These approaches cause difficulties in estuarine and coastal environments, where soft mud beds can deform under normal stresses, changing the relationship between tangential and normal stresses, or where porous beds can experience large (and fluctuating) normal stresses and flow through the bed.

22. For these reasons and the soft beds problems cited in paragraphs 7-9, shear stress exerted on the sediment bed by the flow is an extremely unsatisfactory parameter for sediment transport calculations.

PART III: BOUNDARY LAYERS AND STRESSES DUE TO CURRENTS

Solving for Stresses and Velocities

23. Use of equation set 6 involves selecting a turbulence closure to represent the Reynolds stresses and fluxes and making simplifying assumptions to the degree necessary for the solution method used and suitable for the purpose. Computational difficulty and, more recently, computer cost have forced use of rather extreme simplifications to obtain estimates of shear stresses and velocities, in spite of the loss of realism.

24. To gain an appreciation for how simplification of the equations affects the end result, the following results are presented.

25. Equation 6b can be integrated over width so that spatial variations are considered only in the vertical and longitudinal directions. Integrating, dropping the Coriolis effect, and splitting the pressure term into a surface slope term and a density gradient term yields a two-dimensional (vertical) equation of motion

$$\underbrace{\frac{\partial u_i}{\partial t}}_{A} + \underbrace{u_i \frac{\partial u_j}{\partial x_i}}_{B} = \underbrace{-g_i \frac{\partial \eta}{\partial x_i}}_{C} \underbrace{- \frac{g(x_j - \eta)}{\rho} \frac{\partial \rho}{x_i}}_{D} \underbrace{+ \tau_{sw} (x_i - \eta)}_{E} + \underbrace{\frac{\partial}{\partial x_j} \overline{(-\rho u_j' u_i')}}_{F} \tag{8}$$

where

u = time-mean velocity

x = coordinate direction variable

η = displacement of water surface from mean water level

τ_{sw} = sidewall shear stress

$'$ = an instantaneous turbulent fluctuation of a variable

and A is the unsteadiness term (temporal acceleration), B is the nonuniformity term (convective acceleration), C is the surface slope term, D is the longitudinal density gradient term, and E and F are shear stresses arising from boundary resistance.

26. Evaluation of the relative importance of the terms in Equation 8 can be accomplished by an order of magnitude analysis or by use of experimental data. Abbott (1960) did the former by assuming that the tide could be described as a simple progressive wave. For parameters typical of the Thames River he found that the unsteady and surface slope terms (A and C) were the most important, followed by nonuniform flow and density gradient terms (B and D).

27. An experimental evaluation of the terms in Equation 8 was performed using data from the US Army Engineer Waterways Experiment Station (WES) salinity flume (test 14) in which a 10-min tide of 0.10-ft* amplitude was induced in the ocean headbay (salinity 30 ppt) while a freshwater flow of 0.0075 cfs was introduced at the upstream end of the 327-ft-long, 0.75-ft-wide flume. The vertical salinity gradient in this test was moderate, with about a 30 percent difference between salinities at the bottom and surface at a point 40 ft from the ocean end of the flume.

28. Using a three-point piecewise linear fit (e.g., see Halliwell and O'Connor 1968) to data points in the vertical and difference forms for the derivatives, terms A-D in Equation 8 were evaluated at one station in the salinity flume. Figure 3 shows the individual terms' variation in magnitude plus their sum over a complete cycle. At the bottom of the figure the depth-averaged current velocity and water-surface elevation histories at that station are shown. Terms A-D were nondimensionalized by dividing by ρgh, where h is the mean water depth.

29. As in Abbott's analysis, the surface slope and unsteady terms were the largest, but at times during the cycle the density and nonuniform flow terms became significant in comparison. The nonuniform flow term should not be expected to be large since the flume is prismatic. Using the three-point piecewise fit and considering variation of ρ with respect to y (vertical coordinate) resulted in about a 5 percent reduction in the magnitude of the surface slope terms for the flume data. This suggests that for similar conditions that can be adequately described by linear approximations, the variation of ρ with y may be neglected for individual terms and the total shear except when the direction of flow is reversing. However, these analyses

---

* A table of factors for converting non-SI units of measurement to SI (metric) units is found on page 4.

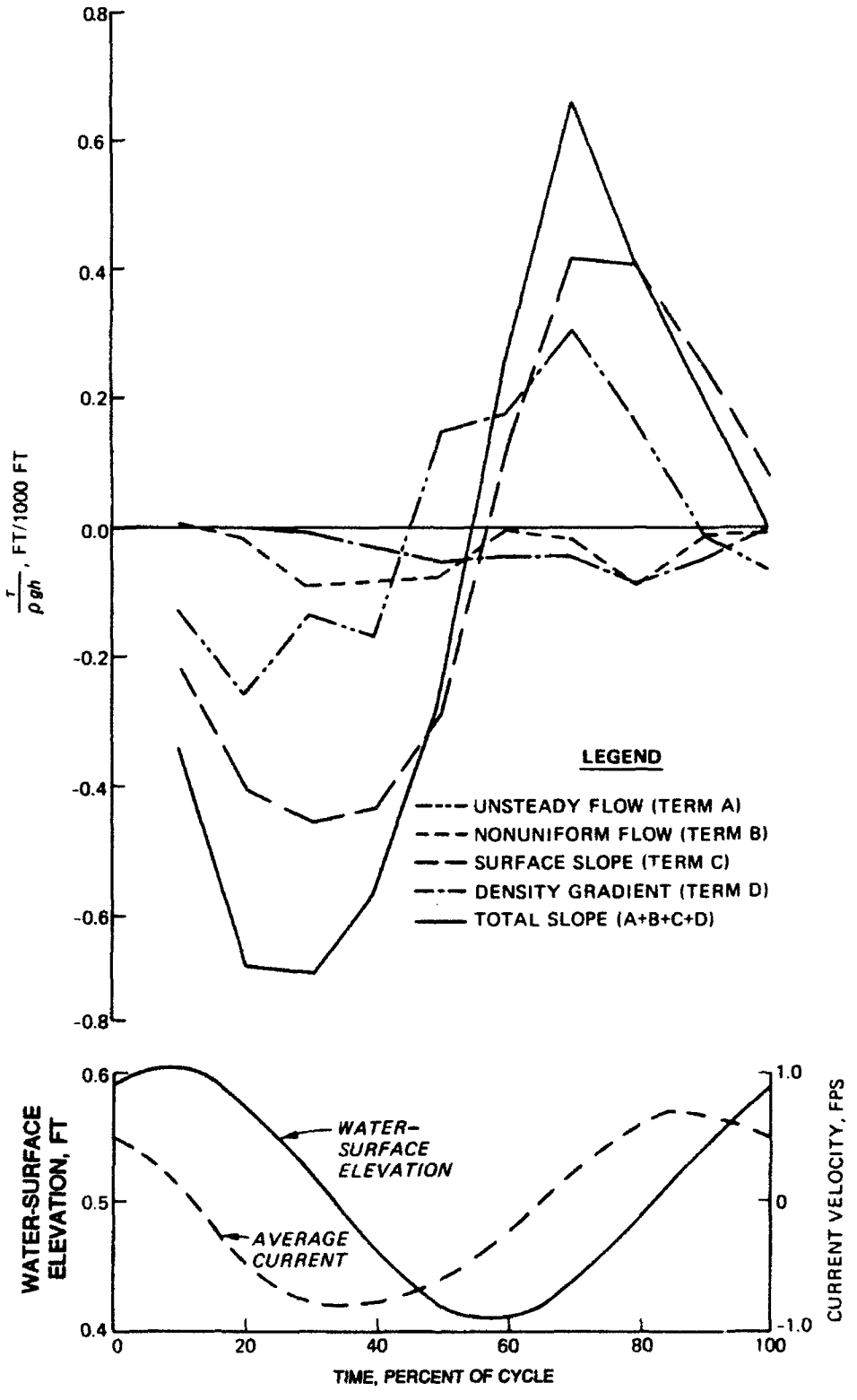

Figure 3. Flume boundary stress contribution by terms A-D

showed that it may not be appropriate to automatically assume further simplifications to Equation 8 for all cases. Rather, for each application an evaluation must be made as to the proper simplifying assumptions.

30. Figure 4 shows how the actual slope is approximated by a typical steady-flow bed shear stress equation of the form

$$\tau = \frac{1}{2} f_c \rho u_1^2 \tag{9}$$

where f_c is a constant friction factor with an empirically derived steady-flow value of 0.02 for the salinity flume, and u_1 is a flow velocity at a specified distance above the bed.

31. Figures 3 and 4 show that, for the fairly simple case of stratified flow in a prismatic flume, using the surface slope or a simple velocity squared equation for calculating the boundary stresses can lead to significantly low magnitude estimates. At small values, even the direction of stress can be in error. In more complicated flows characteristic of natural environments, the errors can be even larger.

Steady, Uniform Flows

32. For steady, constant-density, uniform flows, the coefficient f_c in Equation 9 is equal to one fourth the Darcy pipe flow friction factor f, and when the flow is also rough and turbulent, it can be related to the Chezy C, Manning's n (non-SI units), and effective roughness k_s coefficients by

$$f_c = \frac{2g}{C^2} = \frac{2gn^2}{(1.49R^{1/6})^2} = 0.028 \left(\frac{k_s}{R}\right)^{1/3} = \frac{f}{4} \tag{10}$$

where R is the hydraulic radius.

33. Shear stress can be calculated by Equation 9 with an estimated value of f_c, or by fitting a theoretical profile to observed velocity variation in the vertical. Table 1 shows the commonly used equations in a form that provides an estimate of the roughness coefficient. The Prandtl equations are

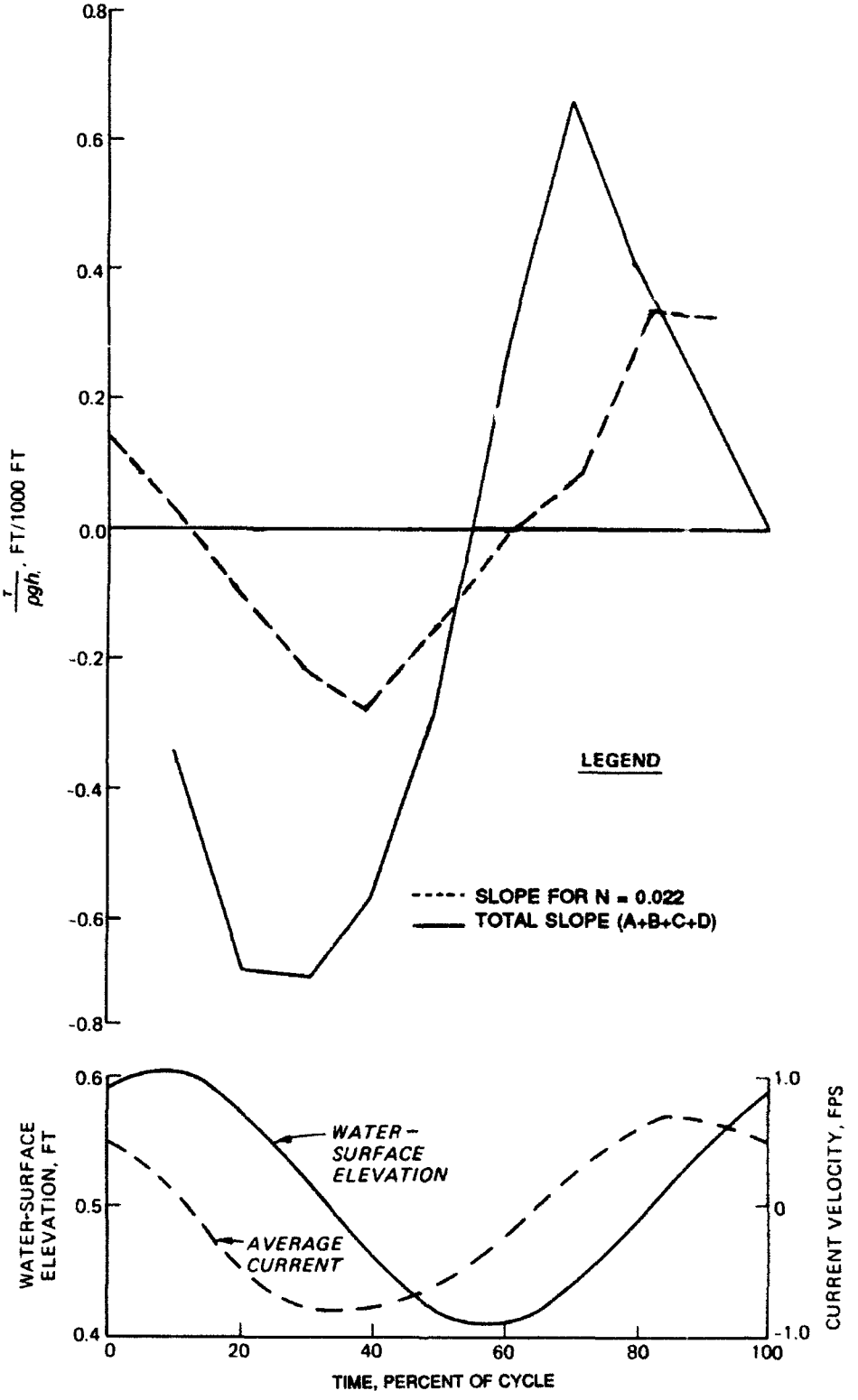

Figure 4. Flume boundary stress by equation of motion and by constant friction factor

limited to the near-wall portion of the boundary layer because of Prandtl's assumption that shear stress in the fluid is not a function of distance from the wall. That restriction is often ignored, but using velocities more than 15 percent of δ (the boundary layer thickness) away from the wall can lead to shear stresses that are too high by significant amounts (Lyles and Woodruff 1972). The corresponding velocity profile equations are as follows:

a. Modified von Karman-Prandtl

$$\frac{u}{u_*} = \frac{1}{\kappa} \ln \left(\frac{y}{k_s} + 0.0338 \right) + 8.5 \tag{11}$$

b. Velocity defect

$$\frac{U_o - u}{u_*} = C_{V1} \log \frac{y}{\delta} + C_{V2} \tag{12}$$

$$C_{V1} = \begin{cases} -5.6 & y < 0.15\delta \\ -8.6 & y > 0.15\delta \end{cases}$$

$$C_{V2} = \begin{cases} 2.5 & y < 0.15\delta \\ 0 & y > 0.15\delta \end{cases}$$

c. Power law

$$\frac{u}{u_*} = 8.74 \left(\frac{u_* y}{\nu} \right)^{1/7} \tag{13}$$

where

y = distance above the bed

U_o = free-stream steady velocity

δ = boundary layer thickness

C_{V1}, C_{V2} = constants

Unsteady, Nonuniform Flows

34. The challenge in solving for turbulent, unsteady, nonuniform flows lies in finding a suitable way to solve for the Reynolds stress and flux terms of Equation 6. In the simplest form, the terms are integrated over space (as in Equation 8) and an expression such as Equation 9 for boundary shear stresses is employed. A somewhat more complicated eddy viscosity approach is used for internal flow stresses and sometimes for boundary stresses as well. (An analogous approach is used for fluxes.) Progressively more complex (and sometimes more realistic) descriptions of the Reynolds terms are attempted through turbulence transport models, sometimes referred to as higher order turbulence closures.

35. The array of possible solutions to the Reynolds terms spans a continuum of complexity and physical realism. Here, that continuum is broken for convenience into steady uniform flow equations, eddy viscosity models, and turbulence transport models. The laminar case is first briefly described, then turbulent flows are considered in more detail.

Laminar flow

36. Schlicting (1968) solved an approximate expression for laminar boundary layer flows that occur when an oscillating current occurs adjacent to a no-slip boundary. Although estuarine flows are rarely laminar, they may be so very near the boundary and near slack water. This simplified case illustrates the behavior of oscillatory boundary layers and gives a starting point for further development.

37. In Schlicting's solution a free-stream velocity of

$$u = U_o \sin \sigma t \tag{14}$$

where

U_o = maximum free-stream velocity

$\sigma = 2\pi/T$, frequency of oscillation

T = period of oscillation

adjacent to a fixed, no-slip boundary results in a near-boundary velocity profile given by

$$u(y,t) = U_o \sin \sigma t \left[1 - e^{-\beta y} (\cos \beta y \sin \sigma t - \sin \beta y \cot \sigma t)\right] \quad (15)$$

where

$$\beta = \sqrt{\sigma/2\nu}$$

Equation 15 is a damped harmonic function in y, the distance away from the boundary. Figure 5 illustrates the form of the profile at various times during T. Note that since the boundary layer velocity overshoots the free-stream velocity, a standard definition of steady-flow boundary layer thickness, such as the distance between the wall and the point at which $u = 0.99U_o$ does not have the same physical significance in the oscillatory case. If the boundary layer is defined as that zone where the velocity differs significantly from the free-stream velocity, the point at which $\beta y = \pi$ is a more appropriate measure. Thus, the oscillatory boundary layer thickness would be expressed as

$$\delta = \pi\sqrt{\frac{\nu T}{\pi}} = \sqrt{\pi \nu T} \quad (16)$$

For laminar flows of tidal periods, this yields a maximum thickness of 1.5 ft.

Turbulent flows

38. The solution for laminar flow (Equation 15) does not extend to boundary layers in turbulent flows. Many researchers have assumed or attempted to show that the boundary layer in oscillatory flow of tidal periods constitutes a considerable portion of the depth of flow. Sternberg (1968) measured Puget Sound tidal velocities at three points within 1 m of the bed and found that velocity profiles at sites with intense flow, complex geometry, and small density gradients could be satisfactorily represented (the curve fit the data points with some scatter) by a logarithmic profile 62 percent of the time. Since the logarithmic portion of the velocity profile (see paragraph 33) is limited to about the lower 15 percent of the boundary layer, a 1-m-thick log layer implies a boundary layer about 5-10 m thick.

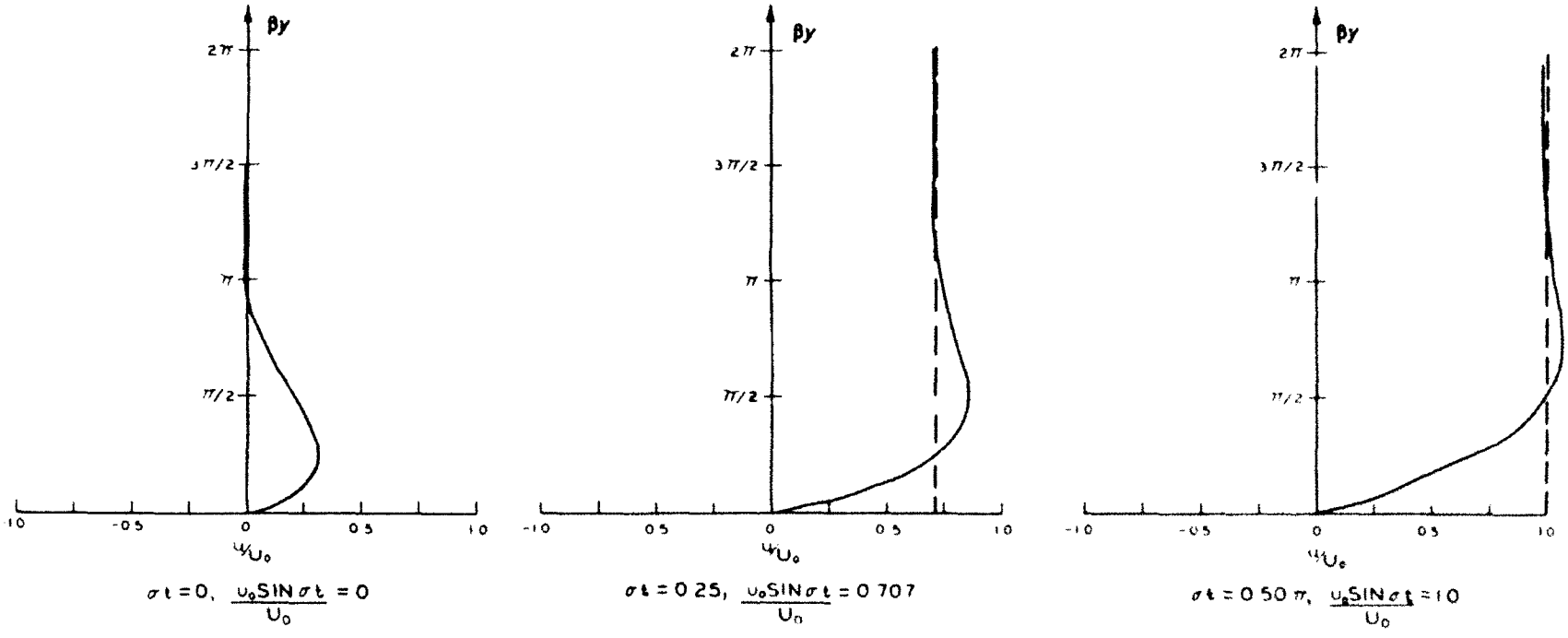

Figure 5. Velocity profile in a laminar oscillatory boundary layer (Continued)

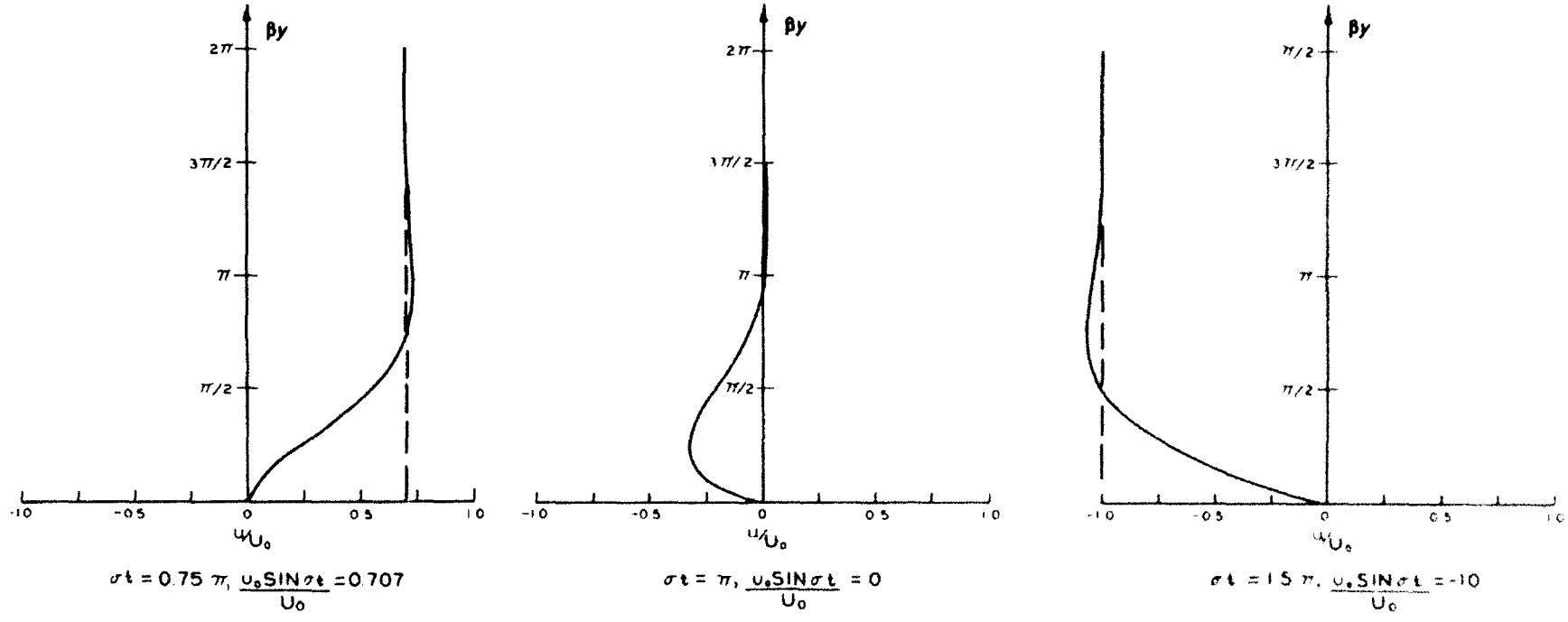

Figure 5. (Concluded)

Lesht (1978), measuring the frequency of turbulent fluctuations and mean flow speed in the New York Bight, found that velocities within 1 m of the bed demonstrated varying degrees of correlation with a log profile, depending largely on the time period over which velocities were averaged. For averaging periods greater than 4 min, the correlation coefficients ranged from 0.55 to 0.90. Lesht attributed low correlation at shorter averaging periods to wind/wave- induced velocity fluctuations.

39. Mehta and Christensen (1977) applied the modified von Karman-Prandtl equation (Equation 11) to flow in tidal inlets using several velocity measurements within 1 m of the bed. They reported a satisfactory fit to the data points by the theoretical velocity profile. Ludwick (1973), assuming the boundary layer thickness to be equal to the flow depth, applied the velocity defect concept (Equation 12) to Chesapeake Bay flows with reasonable results.

40. The presence of vertical or horizontal density gradients further complicates consideration of estuarine velocity profiles. Density gradients distort the velocity profile from that of well-mixed flows, resulting in a tidally averaged circulation pattern like that of Figure 1. At times the near-bed velocity may be in the opposite direction from that of the free stream, due either to phase shifts as shown in the laminar case or to the pressure gradient caused by density differences. Even if we may marginally assume 1-m-thick logarithmic profiles in well-mixed tidal flows, such an assumption is quite often invalid for partially or strongly stratified flows as shown in Figure 1.

Using steady, uniform flow equations

41. Sternberg (1968), using a log profile, calculated values of f_c (Equation 9) for a characteristic velocity 1 m above the bed. He found a mean value of $f_c = 0.0062$, with 95 percent confidence limits of 0.0017 and 0.022. For Reynolds numbers greater than 1.5×10^5, results were less variable and the mean value of f_c was 0.0060.

42. Bowden, Fairbairn, and Hughes (1959) found that reasonable shear stresses resulted from Equation 9 using a value of f_c of 0.007 and a characteristic velocity measured at a distance above the bed equal to 5 percent of the water depth.

43. Though several of these researchers have found that velocity profiles can often be well approximated by a logarithmic profile, it does not necessarily follow that the assumption of a log profile yields a satisfactory

estimate of shear stress. There is usually a great deal of noise in velocity measurements, and any continuous (in space) expression is generated on a best-fit basis to that data. Thus, a theoretical velocity profile may "look" like a satisfactory approximation to the measured velocity points without correctly predicting the shear stress at the bed.

44. Table 2 lists values of f_c obtained by several investigators and those resulting from Equations 10, 11, and 12. Although there is a considerable range between the highest and lowest values, most are equal to about 0.007. As previously mentioned, part of the difficulty in defining f_c from field data is that it is time dependent, in that flow may be changing from hydraulically smooth to hydraulically rough, the bed itself may be changing with time and space, and the pressure gradient dependency of friction (Ludwick 1973; Smith and McLean 1977) is not included. Under these conditions, average shear stresses may be computed from suitably time- and space-averaged velocity profiles, but instantaneous local shear stresses may differ substantially from such averages. It is probable that the field-determined values of f_c are more appropriate for total shear than for bed shear, particularly for noncohesive bed cases. The values in Table 2 suggest that f_c for the flat bed case may be as much as an order of magnitude less than field-derived values. In the absence of better information, one of the forms of Equation 10 can be used for a constant friction coefficient, and an estimate of a time-varying bed surface shear stress can be obtained by multiplying the values from Equation 10 by the cube root of the ratio of k_s based on grain size to an effective total k_s .

Eddy viscosity models

45. Next in complexity after the steady-flow equations come the simple turbulence closure models. They are typically based on a turbulent eddy viscosity coefficient ν_t that is analogous to the kinematic viscosity ν and is used in an expression for shear stress

$$\tau = \nu_t \frac{\partial u}{\partial y} \tag{17}$$

which parallels the expression for laminar shear stress. Knight (1978) and Sleath (1984) provide excellent reviews of these models.

46. The difficulty with this approach is defining an appropriate value for the eddy viscosity. Since it is a property of the flow instead of the fluid (like kinematic viscosity), eddy viscosity is not constant in space or time. In the simplest case it is assumed constant. In progressively more realistic (and computationally more complex) approaches it is assumed to be constant over two or three horizontal layers in the water column. Only one such model is presented here.

47. Three-layer model. Kajiura (1968) proposed a widely cited three-layer model that defines an inner layer next to the bed, an overlap layer, and an outer layer. The eddy viscosity for each layer is given by

$$\nu_{t,inner} = \nu_{t1} = \begin{cases} \nu & \text{for smooth flow} \\ 2.71\,\kappa u_* \delta_1 \end{cases} \tag{18}$$

$$\nu_{t,overlap} = \nu_{t2} = \kappa u_* y \tag{19}$$

$$\nu_{t,outer} = \nu_{t3} = \kappa u_* \delta_o \tag{20}$$

where

$\kappa = 0.4$

δ_1 = inner layer thickness

δ_o = thickness of all three layers

and

$$\delta_o = 0.05\,\frac{u_*}{\sigma} \tag{21}$$

$$\delta_1 = \begin{cases} \dfrac{12\nu}{u_*} & \text{smooth beds} \\ \dfrac{k_s}{2} & \text{rough beds} \end{cases} \tag{22}$$

The overlap layer disappears if $\delta_1 \geq \delta_o$.

48. For an oscillatory free-stream velocity of the form

$$u = U_o \cos \sigma t \tag{23}$$

the equation of motion yields for the boundary layer velocity

$$u = \text{REAL}\left[U_o \left(1 - e^{\alpha_1 y} + A_1 \sinh \alpha_1 y\right) e^{i\sigma t}\right] \tag{24}$$

where

$$A_1 = \frac{(\alpha_1 + \alpha_2) e^{\alpha_1 \delta_o}}{\alpha_1 \cosh (\alpha_1 \delta_1) + \alpha_2 \sinh (\alpha_1 \delta_1)} \tag{25}$$

$$\alpha_1 = \sqrt{\frac{i\sigma}{\nu}} \quad \text{for smooth beds}$$

$$= \sqrt{\frac{i\sigma}{0.185\, \kappa u_* k_s}} \quad \text{for rough beds} \tag{26}$$

$$\alpha_2 = \sqrt{\frac{i\sigma^2}{0.05\, \kappa u_*^2}} \tag{27}$$

and

$$i = \sqrt{-1}$$

From these equations it follows that the bed shear stress is

$$\tau = \nu_t \text{REAL}\left[\alpha_1 U_o \left(A_1 \cosh \alpha_1 y - e^{\alpha_1 y}\right) e^{i\sigma t}\right] \tag{28}$$

Computation of velocity profiles and stresses using Equations 18-28 requires knowledge of the free-stream velocity, oscillation period, and effective

roughness size. Since the equations also include the shear velocity, an iterative solution is required.

49. Mixing length model. Mixing length models return to the Prandtl hypothesis that

$$\nu_t = \ell^2 \frac{\partial u}{\partial y} \tag{29}$$

and rely on one of several expressions for the value of ℓ, the mixing length. One set of expressions commonly used is

$$\ell = \begin{cases} \kappa y \dfrac{40\nu}{u_*} & 0 \le y \le y_1 \\ \alpha_\ell \delta & y_1 \le y \le \delta \end{cases} \tag{30}$$

where α_ℓ and y_1 are empirical parameters.

50. Continuous analytic forms. More recently, eddy viscosity formulations in width-integrated and three-dimensional numerical models have been expressed as a continuous function over depth of a constant form (e.g., parabolic) with a magnitude expressed as a spatially or temporally varying coefficient, such as the following (King 1988):

$$\nu_{txy} = \nu_{tR} \left[A + \frac{y}{h} \left(B + \frac{y}{h} C \right) \right] \tag{31}$$

where

ν_{txy} = spatially and temporally varying eddy viscosity

ν_{tR} = reference value of eddy viscosity

A,B,C = constants

and ν_{tR} is modified by an appropriate factor in stably stratified flows.

51. Reasonably good agreement with field data has been obtained in

San Francisco Bay using this general approach (Cheng, Wang, and Gartner 1988). Equation 31 has been used by King (1988) in the three-dimensional numerical model RMA-10, which has been applied to estuarine flow problems (Richards and Bach 1988; McAnally, Letter, and Thomas 1986) with satisfactory results.

Advantages and disadvantages

52. These steady-flow and simple eddy viscosity approaches offer the advantages of simplicity and relatively small computational effort. They are also entirely adequate for many estuarine applications, including water level and horizontal circulation calculations and even depth-integrated sediment transport where deposition rates are of paramount interest. They are less useful and sometimes possibly misleading when used for vertical circulation, near-bed velocity profiles, and sediment erosion problems. These latter cases require that the simpler approaches be used with extreme caution or that more general methods be used.

53. The eddy viscosity approaches can be modified for some effects (such as stratification) by analytical and empirical methods. These methods are described later in this part.

Stratification Effects

54. Methods of correcting for density stratification (e.g., due to temperature, salinity, and/or suspended sediment) in determination of boundary shear and velocity profiles in surface water flows are necessary if the turbulence calculation method does not explicitly account for it.

55. French (1977) found that in stratified flow the Chezy coefficient C is a function of the Reynolds number, boundary roughness, and density gradient. He started with the basic relationship between C and the shear velocity, u_*,

$$C = \left(\frac{\bar{u}}{u_*}\right)\sqrt{g} \tag{32}$$

where $\bar{u}$ is the average flow velocity. Then he derived the following equation for the vertical velocity gradient in stratified flows using Prandtl's mixing length assumption:

$$\frac{du}{dy} = \frac{\rho u_*^3}{\kappa y\left[\rho u_*^2 - \alpha_f \kappa^2 g y^2 \frac{d\rho}{dy}\right]} \tag{33}$$

where French takes $\alpha_f = 5.0$. Integration of this equation gives the vertical velocity profile $u(y)$ as a function of the vertical density profile $\rho(y)$. Incorporating Equation 33 into Equation 32 gives

$$C = \frac{\sqrt{g}}{h} \int_{y_o}^{h} \frac{u(y)}{u_*} dy \tag{34}$$

where y_o is the bed roughness height. Accounting for the effect of stratification on the velocity profile requires solving Equations 32, 33, and 34 for a given density profile for u_* and iteratively for C and $u(y)$. Comparison of C predicted using Equation 34 with a few experimental data sets indicated good agreement.

56. McCutcheon (1981), following an approach similar to that of French, started with the von Karman-Prandtl law of the wall, incorporated the similarity analysis of Monin and Obukhov, and developed the following formula for the vertical velocity distribution for unidirectional, hydraulically rough, continuously stratified open channel flow:

$$\frac{u(y)}{u_*} = \frac{1}{\kappa} \int_{y_o}^{h} \frac{dy}{y\left[1 + \alpha g \kappa^2 y^2 \left(\frac{f(y)}{\rho_m u_*^2}\right)\right]} \tag{35}$$

where

$f(y) = \partial\rho/\partial y$

$\alpha = r\alpha_f$ with r the ratio of mass mixing length to momentum mixing length

ρ_m = depth-averaged density

Equation 35 can be substituted into the integrand of Equation 34, and then solved for C and u_* in the same manner. McCutcheon performed several

laboratory tests in which salt was the stratifying agent in order to verify Equation 35. One limitation of the methods by French and McCutcheon is that they both assume the law of the wall to be valid over the entire depth of flow. In addition, if the vertical density profile is not known a priori, these equations for the velocity profile would have to be solved coupled with the conservation of mass equation for salt or sediment (Equation 6c).

Turbulence Transport Models

57. Recently, unsteady-flow research has shifted away from use of analytic expressions and constants for eddy viscosity/mixing length and concentrated on various higher level approaches that consider turbulence characteristics in more detail. These approaches aim to develop additional expressions based on constants that are truly constant among a given class of problems (e.g., open channel flow) and not flow dependent. Two basic approaches are given in the literature under a variety of titles. Reviews of the several turbulence transport approaches are available (e.g., Markatos 1986; Task Committee on Turbulence Models in Hydraulic Computations 1988); however, only two are presented here.

58. Turbulence transport models begin with the Eulerian conservation of mass and momentum equations and an equation of state, which are given in Part II as Equation 6.

59. In turbulence transport models, the Reynolds stress and flux terms are expressed in further equations that involve production, transport, and dissipation of turbulent kinetic energy. Two prominent approaches are the $k - \epsilon$ model and the level 2-1/2 model, both described in the following paragraphs.

$k - \epsilon$ model

60. In $k - \epsilon$ models the turbulent kinetic energy k is transported, produced, and dissipated. These models have been widely described and applied (e.g., see Rodi 1982 and 1987). The conservation of turbulent energy equation is expressed as

$$\frac{Dk}{Dt} = \frac{\partial}{\partial x_i}\left(C_{k1}\nu_t \frac{\partial k}{\partial x_i}\right) + P_s + G - \epsilon \qquad (36a)$$

where P_s represents production of turbulence by

$$P_s = \nu_t \left(\frac{\partial u_i}{\partial x_j} + \frac{\partial u_j}{\partial x_i} \right) \frac{\partial u_i}{\partial x_j} \tag{36b}$$

G represents buoyancy contribution to turbulence,

$$G = \frac{1}{\rho_o} g_i \frac{\nu_t}{\sigma_t} \frac{\partial \rho}{\partial x_i} \tag{36c}$$

where

ρ_o = reference density

σ_t = turbulent Prandtl number

ϵ = dissipation of turbulence expressed by

$$\frac{D\epsilon}{Dt} = \frac{\partial}{\partial x_i} \left(C_{\epsilon 1} \nu_t \frac{\partial \epsilon}{\partial x_i} \right) + C_{\epsilon 2} \frac{\epsilon}{k} \left(P_s + C_{\epsilon G} - C_{\epsilon 3} \frac{\epsilon^2}{k} \right) \tag{36d}$$

with ν_t equal to $C_\nu (k^2/\epsilon)$. The notation is the same as in Part II and the C's are constants. If the equations are truly general, the five C's will actually be constant for all flows. Their values are given by Bradshaw, Cebeci, and Whitelaw (1981) and Rodi (1987) as

$$C_\nu = 0.09$$

$$C_{k1} = 1.0$$

$$C_{\epsilon 1} = 0.77$$

$$C_{\epsilon 2} = 1.45$$

$$C_{\epsilon 3} = 1.9$$

The value for $C_{\epsilon G}$ is 1 for positive G and 0 - 0.2 for negative G (Task Committee 1988).

61. The k - ϵ model offers coefficients that are more reliably constant over a given class of flows than are the empirical coefficients of simpler methods by incorporating more physical realism at the cost of sharply increased computational effort. While the transport of turbulent energy seems clearly a more physically reasonable concept than simpler eddy viscosity models, the concept of transporting dissipation is not so clearly reasonable. Were it not for the k - ϵ model's success in reproducing a number of complex

flow fields (Rodi 1987), the concept would seem suspect because of the dissipation equation.

62. More serious deficiencies in the $k - \epsilon$ model are that (a) in its basic form it does not account for flow stratification effects on turbulence and (b) it does not predict the flow field close to solid boundaries well without special adaptation to a law of the wall form.

63. Takemitsu (1988) has proposed a modification to the $k - \epsilon$ model that replaces Equation 36d with

$$\frac{D\epsilon}{Dt} = \frac{\partial}{\partial x_i}\left(C_{\epsilon 1}\nu_t \frac{\partial}{\partial x_i}\right) + C_{\epsilon 2}\frac{\epsilon}{k} P - C_{\epsilon 3}\frac{\epsilon^2}{k} - \frac{\epsilon}{k}\frac{\partial}{\partial x_i}\left(C_{\epsilon 4}\nu_t \frac{\partial k}{\partial x_i}\right) - C_{\epsilon 5}\frac{\nu_t}{\epsilon}\left(\frac{\partial \epsilon}{\partial x_i}\right)^2 + C_{\epsilon 6}\frac{\nu_t}{k}\frac{\partial k}{\partial x_i}\left(\frac{\partial \epsilon}{\partial x_i}\right) - C_\nu C_{\epsilon 7}\left(\frac{\partial k}{\partial x_i}\right)^2 \quad (36e)$$

which increases the number of constants to nine. He specifies the range of constant values as shown in the following tabulation.

Constant	Minimum Value	Probable Value	Maximum Value
C_{k1}	1	3	$0_{(10)}$
C_{k2}	$0.4C_{k1}$	$0.5C_{k1}$	$0.6C_{k1}$
$C_{\epsilon 1}$	1	1	$0_{(10)}$
$C_{\epsilon 2}$	--	2	--
$C_{\epsilon 3}$	--	2	--
$C_{\epsilon 4}$	0	1	$0_{(10)}$
$C_{\epsilon 5}$	1	$C_{\epsilon 1}$	$0_{(10)}$
$C_{\epsilon 6}$	-10	0	2
$C_{\epsilon 7}$	-5	0	5
C_ν	0.065	0.086	0.107

64. Equation 36e is said by Takemitsu to improve the $k - \epsilon$ formulation performance near walls since it includes the effect of diffusion on ϵ. As evidence of its superiority, he shows that in a trial application to open channel flow (using the probable constant values from the tabulation), the resulting eddy viscosity exhibits a minimum at the bed and surface, plus a third minimum at middepth, a reasonable distribution that is not obtained with some approaches. Equation 36e does not include a bouyancy term.

Level 2-1/2 model

65. An alternate approach to turbulence transport modeling is presented by Mellor and Yamada (1982) and endorsed for numerical flow models by Blumberg and Kantha (1986). The level 2-1/2 model describes turbulent kinetic energy by

$$\frac{Dk}{Dt} = \frac{\partial}{\partial x_j}\left[\ell S_q \sqrt{2k}\ \frac{\partial k}{\partial x_j}\right] + P_s + G - \epsilon \tag{37a}$$

where S_q is a constant defined in paragraph 66.

$$P_s = \nu_t \left[\left(\frac{\partial u_i}{\partial x_j}\right)^2 + \left(\frac{\partial u_k}{\partial x_j}\right)^2\right] \tag{37b}$$

$$G = \frac{g}{\rho_o} D_{in} \frac{\partial \rho}{\partial x_j} \tag{37c}$$

where

$$D_{in} = \sqrt{2k}\ \ell S_H \tag{37d}$$

and S_H is defined in Equation 37i, and ϵ is again dissipation but is a rate expressed as

$$\epsilon = \frac{(2k)^{3/2}}{\Lambda_1} \tag{37e}$$

where Λ_1 is a length scale.

66. The level 2-1/2 model also includes an equation for the master mixing length scale ℓ, to which all other length scales are proportional.

$$\frac{D}{Dt}(2k\ell) = \frac{\partial}{\partial x_j}\left[\sqrt{2k}\, S_\ell \frac{\partial}{\partial x_j}(2k\ell)\right] + \ell E_1 (P_s + G) \frac{-(2k)^{3/2}}{B_1}\left\{1 + E_2\left[\frac{\ell}{\kappa(2b - x_j)}\right]^2\right\} \tag{37f}$$

where

$$\nu_t = \sqrt{2k}\,\ell S_M \tag{37g}$$

$$S_M = A_2 \frac{\left[1 - \frac{6A_1}{B_1}\left[\frac{P_s + G}{\epsilon}\right]\right]}{\left[1 - (3A_2B_2 + 18A_1A_2)G_H\right]} \tag{37h}$$

$$S_H = A_1 \frac{\left[1 - 3C_1 - \frac{6A_1}{B_1}\left[\frac{P_s + G}{\epsilon}\right]\right] - S_M(1 - 9A_1A_2G_H)}{G_H(18A_1^2 + 9A_1A_2)} \tag{37i}$$

$$G_H = \frac{-\ell^2}{2k}\frac{g}{\rho_o}\frac{\partial \rho}{\partial x_j} \tag{37j}$$

where

ρ = density

κ = von Karman constant

b = channel width

and the constants and their values are listed as follows:

$$A_1 = 0.92$$

$$A_2 = 0.74$$

$$B_1 = 16.6$$

$$B_2 = 10.0$$

$$C_1 = 0.08$$

$$E_1 = 1.8$$

$$E_2 = 1.33$$

$$S_q = 0.2$$

$$S_\ell = 0.2$$

Level 2 model

67. The complexity of the level 2-1/2 model is daunting; however, the complexity is a problem only to the extent that the computer computations may be too slow (or too expensive) for the purpose. A significantly simplified level 2 model described by Mellor and Yamada (1982) may be appropriate for many applications. The level 2 model begins with the level 2-1/2 model and then neglects the derivative and diffusion of turbulent energy, so that Equation 37a becomes

$$0 = P_s + G - \epsilon \tag{37k}$$

Equation 37f for the length scale is replaced with an algebraic expression

$$\ell = \ell_o \frac{\kappa x_j}{\kappa x_j + \ell_o} \tag{37l}$$

where

$$\ell_o = \alpha \frac{\int_0^\infty |x_j| \sqrt{2k}\, d\, x_j}{\int_0^\infty \sqrt{2k}\, d\, x_j} \tag{37m}$$

where α is a constant approximately equal to 0.01 and Equations 37h and 37i are replaced with

$$S_M = \frac{A_1\left[B_1(\gamma_1 - C_1)\right] - \left[B_1(\gamma_1 - C_1) + 6(A_1 + 3A_2)R_f\right]}{A_2(B_1\ \gamma_1) - \left[B_1(\gamma_1 + \gamma_2) - 3A_1\right]R_f} \tag{37n}$$

$$S_H = 3A_2\ \frac{\gamma_1 - (\gamma_1 + \gamma_2)\ R_f}{1 - R_f} \tag{37o}$$

where

$$\gamma_1 = \frac{1}{3} - \frac{2A_1}{B} \tag{37p}$$

$$\gamma_2 = \frac{B_2}{B_1} + \frac{6A_1}{B_1}$$

and R_f is a flux Richardson number

$$R_f = \frac{-G}{P_s} = \frac{S_H\ g}{S_M \rho_o}\ \frac{\partial \rho}{\partial x_j}\left[\left(\frac{\partial u_i}{\partial x_j}\right)^2 + \left(\frac{\partial u_k}{\partial x_j}\right)^2\right]^{-1} \tag{37q}$$

68. The attractiveness of the $k - \epsilon$ and Mellor-Yamada models is that they incorporate implicitly many of the processes we wish to capture in the calculation of boundary layer flows. One contributing factor that they do not represent is the effect that suspended sediment may have on turbulence damping apart from the density effect.

Suspended Sediment Stratification

69. Coleman (1981) derived an expression for $u(y)$ in uniform,

suspended sediment, stratified, open channel flow using the vertical velocity profile given by Scottron (1967) (notation returns to the x,y,z system):

$$\frac{u}{u_*} = \left(\frac{1}{\kappa} \ln \frac{u_* y}{\nu'} + A\right) - \frac{\Delta u}{u_*} + \left(-\frac{\Pi}{\kappa}\right) \omega \left(\frac{y}{\delta}\right) \tag{38}$$

where

A = integration constant

$\Delta u/u_*$ = channel roughness velocity reduction function (Hinze 1959)

$(\Pi/\kappa)\omega(y/\delta)$ = wake region velocity augmentation function (Coles 1956), where ω is a function of y/δ, and Π is the wake strength coefficient

In Equation 38 ν' is the kinematic viscosity of a solid-liquid two-phase mixture at an elevation y above the bed, given by

$$\nu' = \frac{(1 + 2.5c + 6.25c^2 + 15.62c^3)}{\rho + (\rho_s - \rho)c} \tag{39}$$

where c is the sediment volume concentration and ρ_s is the sediment density. Thus, the effect of suspended sediment on the boundary layer structure is explicit in Equation 38.

70. The first expression in parentheses in Equation 38 is the von Karman-Prandtl law of the wall, while the last two terms have been added as a result of subsequent developments in boundary layer theory and constitute the law of the wake. Coles (1956) stated that this latter law is characterized by a velocity profile at a point of separation (or reattachment), at which the flow is locally a pure wake flow. The wake region in turbulent, fully developed boundary layers is an indication of a large-scale eddy structure that is constrained primarily by inertia rather than by viscosity (as is flow in the viscous sublayer), and therefore is similar to the flow region in a wake. Coles (1956) found the following empirical relationship for ω:

$$\omega \left(\frac{y}{h}\right) = 2 \sin^2 \left(\frac{\Pi}{2} \frac{y}{h}\right) \tag{40}$$

Evaluating Equation 33 at $y/h = 1$ gives the expression for u_{max}, from which the velocity defect law is found to be

$$\frac{u_{max} - u}{u_*} = \left[-\frac{1}{\kappa} \ln\left(\frac{y}{h}\right) + \frac{2\Pi}{\kappa}\right] - \left(\frac{\Pi}{\kappa}\right) \omega\left(\frac{y}{h}\right) \tag{41}$$

Coleman stated that this equation describes the velocity distribution for the entire flow depth except for the viscous sublayer. The terms inside the square brackets are the logarithmic part of the von Karman-Prandtl velocity defect law and an intercept term, respectively. The value of the wake strength coefficient Π can be determined by applying a straight-line fit to the measured data points from the asymptotically logarithmic part of the profile to the high values of y/h, giving

$$\Pi = \frac{\kappa}{2} \left(\frac{u_{max} - u}{u_*}\right)_{y/h=1} \tag{42}$$

71. Coleman (1981) found an empirical relationship between Π and the following form of a gross flow Richardson number (Monin and Yaglom 1971):

$$R_i = \frac{gh(\rho_h - \rho_b)}{\rho_m u_*^2} \tag{43}$$

where ρ_h, ρ_b, and ρ_m are the densities of the sediment-water mixture at the water surface, channel bed, and depth-averaged value, respectively. Thus, for the velocity defect profile given by Equation 36, the suspended sediment distribution (and therefore the effect of sediment-induced stratification) is only implicitly accounted for through the relationship between Π and R_i. Unfortunately, Coleman was not able to verify this empirical relationship that he found from laboratory tests using any other data sets. In addition, the validity of applying the empirical relationship found for ω (given by Equation 40) in all bounded shear flows has not been yet ascertained.

72. With these limitations in mind, to use Coleman's method for

determining $u(y)$ and u_*, given a known suspended sediment profile $c(y)$, Equations 40 and 41 would have to be iteratively solved along with a digitized form of the relationship between R_i and Π.

73. Ordonez (1970) applied an empirical correction to the velocity defect law to account for deviations (particularly in the near-bed zone) of measured velocity profiles in sediment stratified flows from that given by the von Karman-Prandtl velocity defect law. His modified velocity distribution is

$$\frac{u_{max} - u}{u_*} = \frac{1}{\kappa} \ln \left[\frac{y}{h} - \Psi \ln \frac{y}{h} \right] \tag{44}$$

where Ψ is an empirically determined coefficient, the value of which was found to vary between 0.001 and 0.016. Ordonez found a correlation between Ψ and κ, with the latter given by

$$\kappa = \kappa_o \left[\frac{1 + c_m(S - 1)}{1 + 2.5c_o} \right] \tag{45}$$

where

c_m = depth-averaged sediment concentration by volume

c_o = maximum (near-bed) sediment volume concentration

S = sediment specific gravity

The relationship between κ and Ψ is a function of W_s/u_*, where W_s is the sediment fall velocity. Thus to determine $u(y)$ and u_*, Equations 44 and 45, along with the implicit relationship between κ, Ψ, and u_*, have to be solved iteratively.

74. Gust (1976) and Gust and Walger (1976) reported that measurements of mean velocity and suspended cohesive sediment profiles in a tidal channel in the North Sea yielded deviations from the law of the wall in a dilute seawater/clay mineral suspension. The same result was obtained from laboratory experiments in a recirculating flume in which tidal flow of a seawater/clay mixture was simulated. Specifically, deviations from the logarithmic law of the wall were found for $10 < y' < 30$, where $y' = yu_*/\nu$. Gust concluded that the law of the wall cannot be used to compute bed shear stress in clay

suspension flows. Yet he did not present an alternate method for determining the velocity profile, and therefore u_*, in flows with clay suspensions.

75. Gust also found that the measured velocity profiles were very similar to those for drag-reducing polymer flows. Thus, he further concluded that drag reduction was occurring in the clay suspension. He hypothesized that drag reduction was at least partially caused by aggregates of clay particles, which change shape under the action of shear or vorticity in a turbulent flow.

76. Gust and Walger noted the following differences between clear water (Newtonian) flows and clay suspension (non-Newtonian) flows: (a) the viscous sublayer thickness for clay suspensions was about five times larger than that for clear water flows under the same flow conditions; (b) the values of κ obtained from the slopes of measured clay suspension velocity profiles varied between 0.3 to 0.4; (c) the velocities in the logarithmic layer were the same for the two types of flow for "comparable Reynolds numbers"; and (d) u_* values for clay suspension flows were approximately 40 percent less than those obtained for clear water flows.

77. With regard to (b), Gust considered the variation in κ a result of the mean flow experimental error of 5 percent, and not due to the presence of suspended cohesive sediment. Thus, he assumed $\kappa = 0.40$ in his analysis. However, many researchers have found that κ is a function of the rate of turbulent energy dissipation, which in turn is partially governed by the suspended sediment concentration (Einstein and Chien 1954, 1955; Einstein and Abdel-Aal 1972; Hino 1963; Ippen 1971; Wang 1981). Coleman (1981) supported the constancy in the value of κ, and attributed the conclusions arrived at in these studies referenced to the incorrect manner in which the data of Vanoni (1946), Einstein and Chien (1954, 1955) and others were analyzed. Specifically, Coleman stated that the existence of the wake flow region and its effect on the velocity profile were unknown at that time, which led them to erroneously believe that it did not matter to which section of a $u(y)$ versus $\log (y)$ plot a straight line was fit to determine the value of κ.

78. Fortier and Scobey (1926) found that the channel velocities for flows carrying suspended cohesive sediment were greater than for clear water flows. Gust (1976) stated that this observation can be explained in terms of the occurrence of drag reduction as follows: the thicker viscous sublayer, which occurs in a clay suspension, means that the velocities in the logarithmic layer above the viscous sublayer must be greater than those in the same

region in clear water flows to obtain the same critical u_* values necessary for erosion of clay particles from the bed surface, as found in clear water flows.

79. Gust and Southard (1983) studied the structure of two-dimensional equilibrium boundary layer flows using two types of bottoms in a laboratory flume: a movable smooth bed of 0.16-mm quartz sand and a nonmovable concrete bottom with the same equivalent sand roughness. They found that the measured velocity profiles did not follow the universal law of the wall for the flows over the movable bed, in which sand grains were rolling over a smooth sand bed (weak bed load), while they did for the nonmovable bed. Further comparison of the two flows revealed that for the flows over the movable sand bed, (a) the logarithmic layer extended further into the wake region; (b) the flows had a reduced value of $\kappa = 0.32 + 0.04$ (even though the water remained sediment free); (c) the logarithmic layer extended down to the top of the moving sand particles; and (d) the friction diagram showed drag reduction that was Reynolds-number dependent.

80. With regard to the third point, Gust and Southard found that with increasing Reynolds number, the viscous sublayer becomes increasingly weakened, and in fact is eventually replaced by a layer that may be either a "buffer layer, a wake, or even an extension of the overlying logarithmic layer." With regard to the first and third points collectively, they mention that as the number of sand grains in motion increase, the logarithmic layer extends both of its boundaries, with the top one approaching the water surface. With regard to the fourth point, Gust and Southard conjecture that drag reduction is controlled mainly by the bed load. In conclusion, Gust and Southard hypothesize that a new type of wall-bounded shear flow theory is required, one with possibly different momentum transfer processes and a velocity defect region that extends from the top of the moving sand particles to the free surface.

Solution Methods

81. The boundary layer calculations discussed in this Part range from simple but crude to sophisticated but difficult. Equations 9-13 are based on classical steady-flow analyses, and they can be solved analytically if the free-stream velocity and boundary roughness are known. This approach has been

commonly used in field and laboratory studies of estuarine flows, but is known to be deficient under many circumstances and seriously in error in some (e.g., stratification or near times of slack water).

82. A more rigorous, but still analytical solution can be obtained by using a multilayer model like Kajiura's (Equations 18-28) for unsteady flows without complications of density stratification or sediment transport. For real-world solutions, with these complicating factors, it is not presently clear whether the additional rigor of Kajiura's solution is to be preferred over specialized modifications to the steady-flow equations which account for stratification (Equations 32-35).

83. Where computational resources are sufficient and the necessary boundary condition data are available, a higher order turbulence closure is recommended. Both the $k - \epsilon$ model and Mellor-Yamada model are physically rigorous, and have much to recommend them, but the authors favor the levels 2 and 2-1/2 Mellor-Yamada for estuarine boundary flows. Their use requires numerical solution of the equations using approximate methods such as finite differences or finite elements. This necessitates use of a computational mesh with appropriately posed boundary conditions. From numerical experiments reported in the literature, it seems probable that extreme care is required in formulation of the numerical solution (e.g., centering of differences).

PART IV: BOUNDARY LAYERS AND STRESSES DUE TO WAVES AND CURRENTS

84. Most practical estuarine applications involve determination of shear stresses due to both waves and currents. In most estuaries wind-generated surface waves would fall into either the shallow-water or intermediate-water wave classification. Thus, as a wave propagates across the water surface, the wave-induced orbital velocity of water particles near the bed induces a shear stress on the bed surface in addition to the shear caused by quasi-steady tidal currents. Reasonable, first-order approximations to the orbital velocities and particle excursions may be obtained from small amplitude (linear) wave theory. Effects/processes not represented by linear wave theory include wave form asymmetry, net mass transport in the direction of propagation, flow through porous beds, and wave breaking. A brief review of wave mechanics (mainly small amplitude theory) is given next.

Water Wave Mechanics

85. For a small amplitude gravity wave of period T, wave length L, and amplitude a, propagating in a quiescent water body of mean water depth h, the wave length, wave number k, and circular wave frequency σ are defined by

$$L = \frac{gT^2}{2\pi} \tanh (kh) \tag{46}$$

$$k = \frac{2\pi}{L} \tag{47}$$

$$\sigma = \frac{2\pi}{T} \tag{48}$$

where g is the acceleration of gravity. The most restrictive assumption made in linear wave theory is that the wave amplitude is "small" relative to the wave length and water depth. This allows linearization of the kinematic and dynamic surface boundary conditions, which allows the boundary conditions at $y = \eta + h$, where y is the vertical distance coordinate and η is the

displacement of the water surface relative to the mean or quiescent water level, to be applied at $y = h$ (quiescent position of the water surface). To quantify "small," it is required that

$$ak \ll \tanh (kh) \tag{49}$$

86. The horizontal velocity component of water particles beneath a single monochromatic wave u_o as a function of distance above the bottom (i.e., $y = 0$) is given by

$$u_o = \frac{agk}{\sigma} \frac{\cosh (ky)}{\cosh (kh)} \sin (kx - \sigma t) \tag{50}$$

where x is the horizontal distance coordinate and t is time. Thus, the velocity is predicted to vary sinusoidally in time using small amplitude theory. This is not a valid assumption when more than one monochromatic wave field is present and in shallow water where higher harmonics become increasingly dominant.

87. Water particle motion beneath a symmetrical (linear) surface wave follows a closed elliptical path, with the amplitude (one-half the particle excursion) of the major axis (which is in the direction of wave propagation, i.e., x-direction) given as

$$A_o = a \frac{\cosh (ky)}{\sinh (kh)} \tag{51}$$

Both u_o and A_o, the horizontal amplitude, become negligible at depths greater than about one-half a wave length.

88. Shear stresses exerted on the seabed by short-period (i.e., wind-generated) waves have been the subject of substantial research. They are usually expressed in the form of Equation 9, with u_1, the velocity in the x-direction at a specified distance above the bed, being the maximum wave orbital velocity near the bed u_{om}. The wave friction coefficient f_w has been

defined by Jonsson (1965) for hydraulically rough turbulent flow to be

$$\frac{1}{4\sqrt{f_w}} + \log \frac{1}{\sqrt{f_w}} = -0.08 + \log \frac{A_{ob}}{k_s} \tag{52}$$

where A_{ob} is the orbit amplitude at the bed (i.e., Equation 51 evaluated at $y = h$); and k_s is the equivalent bed roughness size. Kamphuis (1975) determined the following explicit approximation for f_w:

$$f_w = 0.4 \left[\frac{A_{ob}}{k_s}\right]^{-0.75} \tag{53}$$

which agrees reasonably well with Equation 52 for $2 < (A_{ob}/k_s) < 100$.

89. Linear wave theory is used in most of the methods presented in this Part to estimate the combined bed shear resulting from the passage of a monochromatic nonbreaking wave and tidal currents. It is pertinent to point out here that simply adding the shear stress due to waves to that due to currents is not adequate for most applications, for the same reason that the sum of squares is not equal to the square of sums.

Laminar Flows

90. Collins (1964) derived the following expression for the near-bed velocity profile in which he assumed that a steady, collinear laminar current was not affected by oscillatory wave-induced motion:

$$u = U_\infty [\cos(kx - \sigma t) - e^{\beta y} \cos(kx + \beta y - \beta t)] \pm \bar{U} [0.4\beta y - 0.04(\beta y)^2] \tag{54}$$

where

u = velocity in the direction of the x-axis

U_∞ = amplitude of the horizontal velocity component just above the wave boundary layer

$\beta = (\sigma/2\nu)^{0.5}$ where ν is the kinematic viscosity of water

$\bar{U}$ = laminar current velocity at $y = 5/(\sigma/2\nu)^{0.5}$

As pointed out by Sleath (1984), this equation is a first-order estimate at best since it linearly superposes the laminar flow and wave shear stress fields.

Turbulent Flows

91. This section discusses bed shear stresses and boundary layer structure in combined low frequency (tidal) and high frequency (wind-generated surface waves) turbulent wave-induced flows. Three methods for determining bed shear stress and boundary layer flow in turbulent, combined wave and current flows are discussed: wave-current friction factors, eddy viscosity approaches, and turbulence modeling.

Bed shear-friction factor approaches

92. Bijker (1966) assumed a log velocity profile for a steady current at an angle to the direction of wave propagation and developed an expression for the resultant shear of

$$\frac{\tau_{wc}}{\tau_c} = 1 + \frac{1}{2g}\left[\frac{p' \kappa C u_{om}}{U}\right]^2 \tag{55}$$

where

τ_{wc} = resultant combined shear due to waves and currents

τ_c = shear due to current only

p' = constant coefficient (given as 0.45)

κ = von Karman's turbulence constant

C = Chezy coefficient

U = mean (depth-averaged) current speed

Swart (1974) found that p' was not a constant, but was the following function of f_w :

$$p' = \left[\frac{f_w}{2\kappa^2}\right]^{0.5} \tag{56}$$

Replacing p' in Equation 55 with Equation 56, and the Chezy coefficient with

the equivalent current friction factor, f_c, from Equation 10 and rearranging yields:

$$\tau_{wc} = 0.5 f_c \rho U^2 + 0.25 f_w \rho u_{om}^2 \tag{57}$$

where ρ is the density of water. Bijker used waves with incidence angles of 75 and 90 deg and a steady current. Since it has been found that the log velocity profile may not be a good description of tidal currents, the use of the log law in Bijker's analysis as well as the use of steady currents in his experiments potentially (at least) limits the usefulness of his results.

93. Jonsson (1966) examined bed shear due to combined waves and currents over plane beds. He used a small collinear current ($U < u_o$) and an energy analysis to find that the instantaneous value of shear stress is equal to

$$\tau_{wc} = 0.5 f_{wc} \rho (U + u_o) \, |u + u_o| \tag{58}$$

where f_{wc}, the friction factor for combined waves and currents, is given by:

$$f_{wc} = \frac{f_w u_{om} + f_c U}{u_{om} + U} \tag{59}$$

with f_w given by Equation 52.

94. Experiments by Brevik and Aas (1980) showed good agreement with Equation 59 for $0 < U/u_{om} < 0.4$. For negative values of U/u_{om} (i.e., waves propagating in the opposite direction of the current), f_{wc} was nearly constant at about 0.35. For values of U/u_{om} greater than 0.4, the computed values of f_{wc} were somewhat lower than that given by Equation 59.

95. Experiments used by Jonsson for verifying Equation 58 were for waves propagating in the direction of the current and for $U < u_o$, as stated in paragraph 93. However, as Equation 58 does not explicitly require the second assumption, it can be extended to the general case (oblique

wave-current interaction) by replacing the squared velocity sum with the square of the resultant velocity due to the superposition of U and u_o. Equation 50 evaluated at $x = 0$ gives

$$u_o = u_{om} \sin(\sigma t) \tag{60}$$

while U and u_o expressed in terms of x- and z-components give

$$U^2 = U_x^2 + U_z^2 \tag{61}$$

$$u_o^2 = u_{ox}^2 + u_{oz}^2 \tag{62}$$

The resultant velocity, u_r, can be expressed as

$$u_r^2 = u_{rx}^2 + u_{rz}^2 \tag{63a}$$

$$= (U_x + u_{ox})^2 + (U_z + u_{oz})^2 \tag{63b}$$

$$= U^2 + u_o^2 + 2(U_x u_{ox} + U_z u_{oz}) \tag{63c}$$

Equation 58 gives an instantaneous value of τ_{wc}; therefore, substituting Equation 63 into Equation 58 and integrating over one wave period yields the average wave- and current-induced bed shear stress:

$$\bar{\tau}_{wc} = \frac{1}{T} \int_0^T \tau_{wc}(t)\, dt \tag{64a}$$

$$= \frac{f_{wc}}{2T} \left[U^2 t + \frac{u_{om}^2}{\sigma} (0.5\sigma t - 0.25 \sin(2\sigma t)) \right] \tag{64b}$$

$$= 0.5 f_{wc} \rho (U^2 + 0.5 u_{om}^2) \tag{64c}$$

Because of the form of Equation 58, Equation 64c cannot be separated into two parts as for Equation 63. It should be noted that there is some evidence that the resultant velocity for a quasi-steady current in the presence of oscillatory currents is not a linear vector sum as given in Equation 63a (George and Sleath 1979). However, the phenomenon is not well enough understood to attempt an alternate approach here.

96. Both Bijker's and Jonsson's methods (Equations 57 and 59, respectively) for calculating the surface shear stress contain the friction factor due to currents only f_c . Unfortunately, as discussed in Part III, there is not a single favored way to compute a time-dependent form of f_c for bed surface shear. If near-bed velocity measurements are available, and one is willing to assume the validity of the log profile, then time-dependent values of f_c can be calculated from the appropriate expression in Table 1. With the lack of any better evidence, it may be necessary to use Equation 10 with a grain size k_s to obtain f_c or to use one of the more rigorous approaches discussed previously, back-calculate f_c , and substitute.

97. O'Connor and Yoo (1988) modified Bijker's model to account for the presence of the wave boundary layer and current/wave interaction, in particular reduction of the current speed. They divided the wave period averaged resultant bed shear into a component parallel to the current, $\langle \tau_b \rangle_p$, and normal to the current, $\langle \tau_b \rangle_n$, with

$$\langle \tau_b \rangle_p = \gamma \bar{\tau}_b \tag{65}$$

and

$$\langle \tau_b \rangle_n = \beta \bar{\tau}_b \tag{66}$$

where $\langle\ \rangle$ is the wave period operator; $\bar{\tau}_b$ is the current-induced time mean bed shear stress; and γ and β are given by

$$\gamma = 0.205 \alpha^{0.75} \mu^{1.25} \sin(2\theta) \tag{67}$$

$$\beta = \alpha^2 \left\{ 1 + [0.36 - 0.14 \cos (2\theta)] \left(\frac{\mu}{\alpha} \right)^{1.5} \right\} \tag{68}$$

where θ is the angle which the orbital wave motion makes with the direction normal to the current; and μ is the relative velocity of maximum wave orbital velocity to the current at y', given by

$$\mu = \left(\frac{f_w}{f_c} \right)^{0.5} \left(\frac{u_{bm}}{U} \right) \tag{69}$$

with u_{bm} as the maximum wave velocity at the top of the wave boundary layer; and y' as the hypothetical elevation above the bed (proposed by Bijker) where a line emanating from the seabed ($y = h$) is tangential to the current-only velocity profile. If the wave- and current-induced velocity profile can be approximated as varying logarithmically, then the level y' is approximately equal to ey_1, where e is the base of natural logarithms, and y_1 is the height above the (theoretical) bed at which the velocity is equal to zero (Bijker 1966).

98. The term α in Equations 67 and 68 is defined as the current velocity reduction factor, which accounts for reduction of current in the wave boundary layer, and is evaluated as

$$\alpha = \left[\beta + \delta \left(\frac{f_w u_{bm}^3}{f_c U^3} \right) \right]^{-1/3} \tag{70}$$

where δ is the boundary layer thickness with

$$\delta = \frac{4}{3\pi} + [0.43 - 0.2 \cos (2\theta)] \left(\frac{\mu}{\alpha} \right)^q \tag{71}$$

and

$$q = 0.1 \cos (2\theta) - 1.9 \tag{72}$$

Obviously, Equation 70 has to be solved iteratively with Equations 68 and 71 for α . O'Connor and Yoo (1988) suggest using a Newton-Raphson method. Comparison of this method with several data sets yielded reasonable agreement.

99. The wave friction factor f_w and current-only friction factor f_c used in Equations 69 and 70 were evaluated by O'Connor and Yoo using the following equations:

$$f_c = 0.016 \left(\frac{h}{k_s}\right)^{-1/3} \tag{73}$$

$$f_w = \exp\left[5.213 \left(\frac{2A_o}{k_s}\right)^{-0.194} - 6.67\right] \quad \text{for } \frac{2A_o}{k_s} > 2.0 \tag{74}$$

$$f_w = 0.12 \quad \text{for } \frac{2A_o}{k_s} < 2.0 \tag{75}$$

Eddy viscosity approaches

100. Methods for determining the instantaneous and wave period averaged bed shear stress or friction coefficient for combined wave and current fields as a function of both time-invariant and time-dependent eddy viscosities are also available. Whenever possible, equations that approximate the actual expressions for bed shear or wave-current friction coefficient are presented for ease of use.

101. Grant and Madsen (1979) presented a method for determining (a) the bed shear stress on a rough bottom under the combined action of waves and currents using a wave-current friction coefficient, and (b) the wave- and current-induced velocity profile both inside and outside the wave boundary layer using a time-invariant two-layer eddy viscosity model. They used the two-layer eddy viscosity model:

$$\nu_t = \begin{cases} \kappa y \, |u_{*_c}| & \text{for } y > \delta_w \\ \kappa y \, |u_{*_{wc}}| & \text{for } y < \delta_w \end{cases} \tag{76}$$

where

ν_t = eddy viscosity

y = height above the bed

$|u_{*c}|$ = magnitude of the time-averaged current shear velocity

δ_w = wave boundary layer thickness

$|u_{*wc}|$ = magnitude of maximum shear velocity due to combined wave and current motion

Thus, u_{*wc} incorporates wave-current interaction effects. The magnitude of the maximum wave- and current-induced bed shear stress τ_{bm} is the usual function of $|u_{*wc}|$:

$$|\tau_{bm}| = \rho\,|u_{*wc}|^2 = \frac{1}{2} f_{wc}\,\rho\alpha\,|u_{om}|^2 \tag{77}$$

where u_{om} is given by the modulus of Equation 57 with $y = h$; and α is given by

$$\alpha = 1 + \frac{|U_a|^2}{|u_o|} + 2\,\frac{|U_a|}{|u_o|}\cos\phi \tag{78}$$

where $|U_a|$ is the magnitude of steady current velocity at a height $y = a$ above the bottom; and ϕ is the angle made by U_a with the wave propagation direction.

102. The implicit equation derived by Grant and Madsen for the wave-current friction factor f_{wc} in Equation 77 is:

$$\left[0.097\left(\frac{k_b}{|A_{ob}|}\right)^{1/2}\frac{K}{f_{wc}^{3/4}}\right]^2 + 2\left[0.097\left(\frac{k_b}{|A_{ob}|}\right)^{1/2}\frac{K}{f_{wc}^{3/4}}\right]$$

$$\left(\frac{V_2}{2\alpha^{1/4}}\right)\cos\bar{\phi}_c = \frac{\alpha^{3/4}}{4} - \frac{V_2^2}{4\alpha^{1/2}} \tag{79}$$

where

k_b = characteristic dimension of the physical bottom roughness

$|A_{ob}| = |u_o|/\sigma$ (excursion amplitude)

K = turbulent kinetic energy

$\bar{\phi}_c$ = angle of the average shear stress

and V_2 is given by the following for small currents relative to wave action:

$$V_2 = (2\pi) \frac{|U_a|}{|u_{bm}|} \left(4 - 3 \sin^2 \bar{\phi}_c\right)^{1/2} \tag{80}$$

When the currents are not small compared to the wave motion, the general form of V_2 (given by Equation 14 in Grant and Madsen (1979)) must be used. The K term in Equation 79 is equal to

$$K = \frac{1}{2\zeta_o^{1/2}} \frac{1}{\left(\text{Ker}^2\, 2\zeta_o^{1/2} + \text{Kei}^2\, 2\zeta_o^{1/2}\right)^{1/2}} \tag{81}$$

where $\zeta_o = k_b/30\ell'$ in which $\ell' = (K\,|u_{*_{wc}}|)/\sigma$ and Ker and Kei are Kelvin functions of zeroth order. The term ℓ' is a measure of the wave boundary layer thickness. Once Equation 79 has been solved for f_{wc}, Equation 77 can be used to evaluate $|\tau_{bm}|$.

103. Tanaka and Shuto (1981) used a one-layer time-invariant eddy viscosity model to derive a linear equation for the wave-current friction coefficient. The eddy viscosity they used is given by

$$\nu_t = \kappa y u_{*_{wc}} \tag{82}$$

104. The bottom shear stress in terms of the eddy viscosity is given by the familiar expression:

$$\tau = \rho \nu_t \frac{\partial u}{\partial y} = \rho k u_{*_{wc}} y \frac{\partial u}{\partial y} = \frac{1}{2} \rho f_{wc} u_{bm}^2 \quad \text{at } y = y_o \tag{83}$$

where y_o is the roughness height and $u = u_c + u_w$, the linear combination of the boundary layer velocity profile due to currents and waves. Equations for u_c and u_w are given by Tanaka and Shuto. They derive an approximate (simplified) implicit equation for f_{wc} on a rough bed that is valid for $u_{bm}/\sigma y_o > 50$:

$$f_{wc} = 2B \left(\frac{u}{u_{bm}}\right)^2 + 4BC \left(\frac{u}{u_{bm}}\right) \cos \phi + C^2 \tag{84}$$

with

$$B = \frac{\kappa}{\ln\left(\frac{h}{y_o}\right) - 1} \tag{85}$$

$$C = \frac{\kappa}{\pi} \left\{ 0.25 + 0.101 \left[\ln\left(\frac{y_o}{u_{bm}}\right) - 0.5 \ln (f_{wc}) + 2.42 \right]^2 \right\}^{-1/2} \tag{86}$$

105. Tanaka and Shuto also derive an expression for f_{wc} that is valid for wave- and current-induced turbulent flows over smooth beds:

$$f_{wc} = 2F^2 \left(\frac{u}{u_{bm}}\right)^2 + 4FG \left(\frac{u}{u_{bm}}\right) \cos \phi + G^2 \tag{87}$$

with

$$F = 0.4 \left[\ln\left(\frac{u_{bm} a_m}{\nu}\right) \frac{h}{a_m} \sqrt{f_{wc}} + 0.852 \right]^{-1} \tag{88}$$

$$G = \frac{0.4}{\pi} \left\{ 0.25 + 0.101 \left[2 \ln\left(\frac{1}{\sqrt{f_{wc}}}\right) - \ln\left(\frac{u_{bm} a_m}{\nu}\right) + 0.568 \right]^2 \right\}^{-1/2} \tag{89}$$

where $a_m = 2A_o$. For the smooth bed formulation, the thickness of the viscous sublayer was used in place of the roughness height. Measured wave- and current-induced shear stresses in a laboratory flume showed fairly good agreement with those predicted using Equation 83.

106. Tanaka, Chian, and Shuto (1983) extended the work of Tanaka and Shuto (1981) by using a time-invariant two-layer eddy viscosity model. They used the following two-layer formulation suggested by Mellor and Gibson (1966):

$$\nu_t = \begin{cases} \kappa y u_{*_{wc}} & \text{for } 0 < y < d \\ \kappa d u_{*_{wc}} & \text{for } d < y < h \end{cases} \tag{90}$$

where d is the height of the inner layer. Wave-current interactions were limited to opposing currents (ϕ of 180 deg) and favorable currents (ϕ of 0 deg).

107. There are two basic differences between this work and that of Grant and Madsen (1979): (a) the eddy viscosity as given by Equation 90 is continuous across the interface between the inner and outer layers; and (b) the effect of a steady current is included in determining the height of the inner layer, whereas it was not explicitly accounted for in the work by Grant and Madsen.

108. The expression derived by Tanaka, Chian, and Shuto for f_{wc} using the two-layer eddy viscosity model is very complicated compared with that obtained with the one-layer model (Equation 84), and yet the difference between the two models (for resulting f_{wc}) is insignificant. In addition, comparison of predicted velocity profiles using the one-layer and two-layer models with profiles measured in a wind tunnel showed that in most cases profiles predicted by the one-layer model were closer to the measured profile than those obtained with the two-layer model.

109. Madsen and Wikramanayake (1988) presented an analytical model for turbulent wave-current bottom boundary layer flow using a three-layer time-invariant eddy viscosity formulation. They started by linearizing the two-dimensional (vertical plane) boundary layer equations for an incompressible homogeneous fluid over a plane boundary using an order-of-magnitude

analysis. Next, by expressing u (horizontal flow velocity) and p (pressure) as the sum of time-invariant (current) and time-varying (wave) components, they separated the linearized boundary layer equation into the following two equations for small-amplitude, monochromatic progressive waves and a steady current, respectively:

$$\frac{\partial \vec{u}_w}{\partial t} = \frac{-1}{\rho} \nabla p_w + \frac{\partial}{\partial y} \left[\nu_t \frac{\partial \vec{u}_w}{\partial y} \right] \tag{91}$$

$$0 = \frac{-1}{\rho} \nabla p_c + \frac{\partial}{\partial y} \left[\nu_t \frac{\partial \vec{u}_c}{\partial y} \right] \tag{92}$$

where ∇p is the mean pressure gradient.

110. Madsen and Wikramanayake then assumed a complex harmonic function solution for the linear wave boundary layer equation (Equation 91) and derived the following equation for the wave-induced orbital velocity u_d within the wave boundary layer:

$$\frac{d}{dy} \left[\nu_t \frac{du_d}{dy} \right] - i\sigma u_d = 0 \tag{93}$$

where u_d is a complex function of y and i is $\sqrt{-1}$.

111. Integration of Equation 93 from the bottom ($y \simeq 0$), where $\nu_t(\partial u/\partial y) = \tau_c/\rho$, to a level y yields

$$\nu_t \frac{du_c}{dy} = \frac{\tau_c}{\rho} + \left| \nabla \left(\frac{p_c}{\rho} \right) \right| y \tag{94}$$

The pressure gradient term on the right-hand side of this equation is then dropped as it is small relative to τ_c/ρ , which results in the law of the wall for the equation governing the current boundary layer:

$$\nu_t \frac{du_c}{dy} = \frac{\tau_c}{\rho} = u_{*_c}^2 \tag{95}$$

with u_{*_c} as the shear velocity associated with the current boundary shear stress.

112. Madsen and Wikramanayake (1988) represented the time-invariant eddy viscosity term included in Equations 93 and 95 using the following formulation:

$$\nu_t = \begin{cases} \kappa u_{*_{wc}} y & y \le \alpha_t \delta \\ \kappa u_{*_{wc}} \alpha_t \delta & \alpha_t \delta \le y \le \dfrac{\alpha_t \delta}{\epsilon} \\ \kappa u_{*_c} y & \dfrac{\alpha_t \delta}{\epsilon} \le y \end{cases} \tag{96}$$

where

α = fraction of the wave boundary layer thickness over which the eddy viscosity varies linearly

δ = scale of the wave boundary layer thickness

$\epsilon = u_{*_c}/u_{*_{wc}}$, which represents the relative magnitude of the current turbulence intensity to the combined wave-current turbulence intensity

These definitions will apply to the discussion of Madsen and Wikramanayake's method in paragraphs 112-121. The advantages of this three-layer eddy viscosity model over the two-layer models previously discussed are that (a) it is a continuous function in y, and (b) it is applicable for both weak and strong current-wave interactions.

113. After incorporating Equation 96 into Equation 93, the latter is solved for the three domains specified in Equation 96. The solution for the near-bottom ($y < \alpha\delta$) domain is

$$u_d = A\left[\text{Ker}\left(2\sqrt{\zeta}\right) + i\,\text{Kei}\left(2\sqrt{\zeta}\right)\right] + B\left[\text{ber}\left(2\sqrt{\zeta}\right) + i\,\text{bei}\left(2\sqrt{\zeta}\right)\right] \tag{97}$$

where Ker , Kei , ber , and bei are Kelvin functions of zeroth order; $\zeta = y/\delta$, with $\delta = Ku_{*_{wc}}/\sigma$; and A and B are arbitrary complex constants (to be specified by boundary conditions later).

114. For the intermediate domain ($\alpha\delta < y < \alpha\delta/\epsilon$), the solution of Equation 93 is

$$u_d = C\, e^{\sqrt{i}/\alpha\zeta} + De^{-\sqrt{i}/\alpha\zeta} \tag{98}$$

where $\sqrt{i} = (1 + i)/\sqrt{2}$; and C and D are complex constants.

115. For the outer domain ($y > \alpha\delta/\epsilon$), the solution of Equation 93 is

$$u_d = E\left[\mathrm{Ker}\left(2\sqrt{\zeta/\epsilon}\right) + i\ \mathrm{Kei}\left(2\sqrt{\zeta/\epsilon}\right)\right] + F\left[\mathrm{ber}\left(2\sqrt{\zeta/\epsilon}\right) + i\ \mathrm{bei}\left(2\sqrt{\zeta/\epsilon}\right)\right] \tag{99}$$

where E and F are complex constants.

116. The conditions applied to Equations 97-99 are the no-slip conditions at $y = y_o = k_s/30$, the approach to the free-stream velocity as $y \to \infty$, and matching conditions between the three domains. Applying these conditions resulted in the following five linear equations:

$$A\left[\mathrm{Ker}\left(2\sqrt{\zeta_0}\right) + i\ \mathrm{Kei}\left(2\sqrt{\zeta_0}\right)\right] + B\left[\mathrm{ber}\left(2\sqrt{\zeta_0}\right) + i\ \mathrm{bei}\left(2\sqrt{\zeta_0}\right)\right] = -u_b \tag{100}$$

$$A\left[\mathrm{Ker}\left(2\sqrt{\alpha}\right) + i\ \mathrm{Kei}\left(2\sqrt{\alpha}\right)\right] + B\left[\mathrm{ber}\left(2\sqrt{\alpha}\right) + i\ \mathrm{bei}\left(2\sqrt{\alpha}\right)\right] \tag{101}$$
$$= C\, e^{\sqrt{i\alpha}} + D\, e^{-\sqrt{i\alpha}}$$

$$C\, e^{\sqrt{i\alpha}/\epsilon} + D\, e^{-\sqrt{i\alpha}/\epsilon} = E\left[\mathrm{Ker}\left(2\sqrt{\alpha}/\epsilon\right) + i\ \mathrm{Kei}\left(2\sqrt{\alpha}/\epsilon\right)\right] \tag{102}$$

$$A\left[\mathrm{Ker}'\left(2\sqrt{\alpha}\right) + \mathrm{Kei}'\left(2\sqrt{\alpha}\right)\right] + B\left[\mathrm{ber}'\left(2\sqrt{\alpha}\right) + i\ \mathrm{bei}'\left(2\sqrt{\alpha}\right)\right] \tag{103}$$
$$= C\, e^{\sqrt{ie}\sqrt{i\alpha}} - D\, e^{-\sqrt{ie}\sqrt{i\alpha}}$$

$$C\, e^{\sqrt{ie}\sqrt{i\alpha}/\epsilon} - D\, e^{-\sqrt{ie}\sqrt{i\alpha}/\epsilon} = E\left[\mathrm{Ker}'\left(2\sqrt{\alpha}/\epsilon\right) + i\ \mathrm{Kei}'\left(2\sqrt{\alpha}/\epsilon\right)\right] \tag{104}$$

where u_b is the near-bottom velocity. These five equations can be solved for the constants A, B, C, D, and E once the following five parameters are specified:

$$k_s\ ,\ u_b\ ,\ \alpha\ ,\ u_{*_c}\ ,\ u_{*_{wc}} \tag{105}$$

Madsen and Wikramanayake assume that k_s , u_b , and u_{*_c} are either known or specified, which leaves $u_{*_{wc}}$ and α to be determined. They regard α as a "free (fitting) parameter," and uses a closure hypothesis to determine $u_{*_{wc}}$.

117. The closure hypothesis Madsen and Wikramanayake used assumes that

$$u_{*_{wc}} = \sqrt{\tau_w/\rho} \tag{106}$$

with τ_w the maximum combined wave-current bed shear stress vector expressed by

$$\tau_m = |\vec{\tau}_m| = \left(\tau_w^2\, \tau_c^2 + 2\tau_c\tau_w \cos\phi_{wc}\right)^{1/2} = \tau_w\left(1 + 2\mu^2 \cos\phi_{wc} + \mu^4\right)^{1/2} \tag{107}$$

where

τ_w = maximum wave bottom shear stress

τ_c = average current bottom shear stress at an angle ϕ_{wc} to the wave direction

$\mu = u_{*_c}/u_{*_w}$, and thus equal to the relative magnitude of current to wave bottom turbulence intensity

Combining Equation 107 and the definitions for ϵ and μ yields

$$\epsilon = \left(1 + 2\mu^2 \cos \phi_{wc} + \mu^4\right)^{-1/4} \tag{108}$$

118. Madsen and Wikramanayake define a wave friction factor, f_{wc}, using Equation 10 with $\tau = \tau_w$, and $u_1 = u_b$, and a modified wave friction factor, f'_{wc}, defined to be

$$f'_{wc} = f_{wc}\left(1 + 2\mu^2 \cos \phi_{wc} + \mu^4\right)^{-1/2} \tag{109}$$

Madsen and Wikramanayake obtain the following implicit relationship for the modified friction factor:

$$\sqrt{f_{wc}} = \frac{\sqrt{2\kappa}}{u_b}\sqrt{\zeta_0}\ \left|A\left[\mathrm{Ker}'\left(2\sqrt{\zeta_0}\right) + i\ \mathrm{Kei}'\left(2\sqrt{\zeta_0}\right)\right]\right. \tag{110}$$

$$\left. + B\left[\mathrm{ber}'\left(2\sqrt{\zeta_0}\right) + \mathrm{bei}'\left(2\sqrt{\zeta_0}\right)\right]\right| \quad \text{for limit } \zeta = \zeta_0$$

in which

$$\zeta_0 = \frac{k_n/30}{\kappa u_{ewc}/\sigma} = \frac{k_n/30}{\kappa u_{ew}\frac{\left(1 + 2\mu^2 \cos \phi_c + \mu^4\right)^{\frac{1}{4}}}{\sigma}} = \frac{\sqrt{2}}{30\kappa}\frac{k_n}{A_b}\frac{1}{\sqrt{f'_{wc}}} \tag{111}$$

where k_n is the boundary roughness size
and

$$A'_b = \frac{u_b}{\sigma}\left(1 + 2\mu^2 \cos \phi_{wc} + \mu^4\right)^{1/2} = A_b\left(1 + 2\mu^2 \cos \phi_{wc} + \mu^4\right)^{1/2} \tag{112}$$

119. The current problem (Equation 92) is solved and the no-slip bottom

boundary condition and matching conditions between the three regions are applied to obtain

$$u_c = \frac{u_{*c}}{u_{*wc}} \frac{u_{*c}}{\kappa} \ln \frac{y}{y_0} \quad \text{for } y < \alpha\delta \tag{113}$$

$$u_c = \frac{u_{*c}}{u_{*wc}} \frac{u_{*c}}{\kappa} \left[\frac{y}{\alpha\delta} - 1 + \ln \frac{\alpha\delta}{y_0}\right] \quad \text{for } \alpha\delta < y < \alpha\delta/\epsilon \tag{114}$$

$$u_c = \frac{u_{*c}}{\kappa} \left[\ln \left(\frac{y}{\alpha\delta/\epsilon}\right) + 1 + \frac{u_{*c}}{u_{*wc}} \left[\ln \frac{\alpha\delta}{y_0} - 1\right]\right] \quad \text{for } y > \alpha\delta/\epsilon \tag{115}$$

Madsen and Wikramanayake (1988) point out that the solution for the outer region (Equation 115) is limited by the validity of the law of the wall, and thus should not be used for y greater than a fraction of the current boundary layer thickness.

120. Madsen and Wikramanayake (1988) outline an iterative technique for solving the wave-current problem. The procedure involves initially assuming that u_{*_c} is much smaller than u_{*_w} and u_{*wc}. Thus, in the limit, both μ and ϵ are equal to zero. Equations 110-112 are used to determine the value of f'_{wc}, and then f_{wc} from Equation 109. Using this value of f_{wc}, τ_w is determined using Equation 10, from which new estimates of μ and ϵ are obtained using the definition for μ and Equation 108. These new values for μ and ϵ then replace the original estimates for these parameters in the iterative procedure described previously. Iteration proceeds until convergence is achieved. A value for α is assumed in this method. Then the solution to the wave-current problem can be obtained by solving Equations 100-104 (with the calculated values for μ, ϵ, u_{*wc} and δ) for the wave problem and Equations 112-115 for the current problem.

121. Madsen and Wikramanayake (1988) compared the results from their analytical model with those obtained by Davies, Soulsby, and King (1988) (discussed in the next section) using a numerical turbulence closure model. Excellent comparison was achieved with a value of α of 1/2. This is particularly significant considering the relative simplicity of Madsen and Wikramanayake's model as compared with the full-scale turbulence closure model

developed by Davies, Soulsby, and King.

122. The largest difference seen between the results of Madsen and Davies was that the former showed much less sensivity to the angle between the direction of wave propagation and the current than the latter. For this reason, Madsen has initiated development of a time-varying eddy viscosity model (Madsen and Wikramanayake 1988). This model has not yet been completed.

123. Lavelle and Mofjeld (1983) developed a flow-eddy viscosity interdependent model of the bottom boundary layer using a time-varying eddy viscosity. While their model does not include effects of combined wave motion and currents, they did evaluate the model for the case of oscillatory flow at tidal frequencies. They found that if time variations in the eddy viscosity are neglected, then the maximum bed shear stress is underestimated and the velocity profile is distorted, particularly near flow reversal. Some aspects of their model are described in the following paragraphs.

124. The time-variant eddy viscosity used had the form:

$$\nu_t = \begin{cases} \kappa y |u_b^*(t)| & \text{for } y_o < y < \delta \\ \kappa \delta |u_b^*(t)| & \text{for } y > \delta \end{cases} \tag{116}$$

where

δ = log layer thickness

$u_b^*(t)$ = magnitude of modified shear velocity, given by:

$$|u_b^*(t)| = \left[u_*^2(t) + \nu_t\, u_*^2(t + T/4)\right]^{1/2} \tag{117}$$

where u_* is the shear velocity defined by:

$$u_* = \frac{\tau_b}{|\tau_b|^{1/2}} \tag{118}$$

The bed shear τ_b as a function of time is evaluated using the first expression on the right-hand side of Equation 83.

125. One result from Lavelle and Mofjeld's model was that τ_b and U_o, the free-stream velocity, are not in phase. They presented the following equation for τ_b that incorporates the relative phasing of τ_b and U_o, and both linear and quadratic friction laws:

$$\tau_b(t/T) = g_\beta |U_o(t/T + \theta)|^\beta U_o(t/T + \theta) \tag{119}$$

where θ is the fraction of the wave (tide) cycle between the zeros of τ_b and U_o; β has a value between 0 and 1 (e.g., when $\beta = 1$, τ_b is quadratic in U_o); and g_β is a coefficient (e g., g_β is analogous to C_D (drag coefficient) when $\beta = 1$). The bottom friction was also found to be (implicitly) dependent on the degree of temporal variation of the eddy viscosity.

126. Lavelle and Mofjeld also found that flow acceleration and deceleration cause the steady state near-bed log velocity profile to be modified. Their theoretical near-bed velocity function contains additional terms in $y \ln (y/y_o)$ and y. Soulsby and Dyer (1981) confirm this finding. This emphasizes the previously stated finding that use of conventional log velocity profiles to fit accelerating flow measurements may result in inaccurate estimates of the shear velocity and bottom roughness. This also points out possible limitations of the previous methods reviewed in this section, since most use a log velocity profile for the steady current.

Turbulence modeling approaches

127. The authors recommend the five papers on "Turbulence Modeling of Surface Water Flow and Transport" which appear in the August 1988 American Society of Civil Engineers Journal of Hydraulic Engineering. These papers review the state of turbulence modeling, and thus would greatly benefit the reader in assessing the material discussed herein. Another recommended paper is that of Mellor and Yamada (1982), which was discussed in Part III. As it is beyond the scope of this report to summarize all the material included in even these six papers mentioned, the discussion that follows is limited to a description of one turbulence closure model that has been used to specifically model nonstratified wave- and current-induced boundary layer flow. The model reviewed is not the most complete or advanced, certainly not the most numerically sophisticated; nevertheless, it is able to reproduce known oscillatory

boundary layer structure using a seemingly far less complicated scheme. As such, it appears to be particularly attractive for inclusion in a full-scale three-dimensional turbulence model. Two closure models that account for sediment stratification are reviewed in the next section.

128. Davies, Soulsby, and King (1988) describe a relatively simple turbulence closure model of oscillatory rough-turbulent boundary layer flow that is used to model wave-current interaction in the near-bed zone. The philosophy used by Davies, Soulsby, and King was "to model the flow in a way no more complicated than can be warranted by present abilities to make controlled field measurements." Advantages and features of their approach over similar models include the following: (a) it can be applied to any wave-current condition, from large waves on a weak current to small waves on a strong current; and (b) the turbulence closure scheme involves no new assumptions other than those that have been used in separately modeling wave and current boundary layers.

129. Several assumptions are incorporated in the model: (a) the flow is horizontally uniform between the flat rough bed and horizontal water surface; (b) there is no surface shear stress; (c) boundary layer approximation ($k\delta_{wc} \ll 1$) is valid; and (d) waves have a small amplitude and satisfy the Stokes condition ($ka \ll 1$). This last assumption allows for neglecting the convective acceleration terms in the momentum equations.

130. The following procedure is used in the model to initialize boundary layer flow: (a) a steady uniform starting current is generated; (b) wave motion of a given frequency and incident (with respect to the current direction) angle is then superposed on the current; and (c) the model is run to allow convergence to the combined wave-current steady state. The justification given for starting with a steady current is that it provides consistent initial vertical profiles for velocity and turbulence parameters.

131. The linearized horizontal momentum equation in the z-direction (current direction) that is solved to generate the starting current is

$$\frac{\partial w}{\partial t} = -\frac{1}{\rho}\frac{\partial p}{\partial z} + \frac{\partial}{\partial y}\left[\frac{T_{yz}}{\rho}\right] \tag{120}$$

where $w(y,t)$ is the mean velocity component in the z-direction, and T_{yz} is

the Reynolds shear stress in the z-direction associated with the current. The latter is given by

$$T_{yz} = \rho \nu_t \frac{\partial w}{\partial y} \tag{121}$$

where $\nu_t(y,t)$ is determined, as described in the following paragraphs, using a turbulence closure approach.

132. The following two-dimensional momentum equations are used to superpose wave motion on the steady current:

$$\frac{\partial u}{\partial t} = - \frac{1}{\rho} \frac{\partial p}{\partial x} + \frac{\partial}{\partial y} \left[\frac{\tau_{yx}}{\rho} \right] \tag{122}$$

$$\frac{\partial w}{\partial t} = - \frac{1}{\rho} \frac{\partial p}{\partial z} \frac{\partial}{\partial y} \left[\frac{\tau_{yz}}{\rho} \right] \tag{123}$$

where τ_{yx} and τ_{yz} are components of the shear stress in the x and z directions, given by

$$\tau_{yx} = \rho \nu_t \frac{\partial u}{\partial y} \qquad \tau_{yz} = \rho \nu_t \frac{\partial w}{\partial y} \tag{124}$$

133. The pressure gradients in Equations 122 and 123 are chosen to yield the wave motion specified in the following equations in the region above the wave-current boundary layer (i.e., $y > \delta_{wc}$):

$$- \frac{1}{\rho} \frac{\partial p}{\partial x} = \frac{dU_x}{dt} \qquad \text{with } U_x = U_o \sin \phi \cos (\sigma t) \tag{125}$$

$$- \frac{1}{\rho} \frac{\partial p}{\partial z} = \frac{dU_z}{dt} + \nabla p \qquad \text{with } U_z = U_o \cos \phi \cos (\sigma t) \tag{126}$$

where

U_x, U_z = horizontal water particle velocity components

$U_o = A_o\sigma$

134. In the solution to Equations 122-126 (together with appropriate boundary conditions), to add waves to the already established steady current, ∇p was set equal to a constant. The model was run until the new wave-current equilibrium was achieved. Davies, Soulsby, and King (1988) mention that setting ∇p equal to a constant is not consistent with the assumed horizontal water surface. However, they add that the pressure gradients of concern are usually at least two orders of magnitude smaller than the gradients associated with waves. Therefore, the implied surface slope is negligible and can be thought of as an artifact of the numerical scheme.

135. The turbulence closure scheme Davies, Soulsby, and King used to solve for $\nu_t(y,t)$ is described in detail by King, Davies, and Soulsby (1985). The equation for turbulent energy is given by:

$$\frac{K}{t} = \nu_t \left(\frac{\partial u}{\partial y}\right)^2 + \left(\frac{\partial w}{\partial y}\right)^2 + \alpha' \frac{\partial}{\partial y} \nu_t \frac{\partial K}{\partial y} - \epsilon \tag{127}$$

where $K(y,t)$ is the turbulent energy and α' is the ratio of eddy diffusivities of turbulent energy K and momentum.

136. The boundary conditions for Equation 127 represent zero energy flux across the water surface and bed surface. The turbulence closure scheme is closed using turbulence scaling laws for ν_t and ϵ :

$$\nu_t = c_o \ell K^{1/2} \qquad \epsilon = \frac{c_1 \kappa^{3/2}}{\ell} \tag{128}$$

where c_o and c_1 are constants and ℓ is the mixing length, given by

$$\ell = -\kappa \frac{K^{1/2}}{\ell} \frac{\partial}{\partial y} \left(\frac{K^{1/2}}{\partial} - 1\right) \tag{129}$$

137. For the steady state starting current, Equations 120, 121, and

127–129 are solved together, while for the superposition of waves and currents, Equations 122–129 are solved. A log linear depth transform was applied to these equations, after which Equations 120, 122, 123, and 127 were solved iteratively using an implicit Crank–Nicholson scheme. The convergence criterion was based on the predicted ν_t distribution. Davies, Soulsby, and King (1988) used the values given by Vager and Kagan (1969) for the constants in Equations 120–129: $c_o = c^{1/4}$ and $c_1 = c^{3/4}$, with $c = 0.046$, $\alpha = 0.73$, and $\kappa = 0.4$. King, Davies, and Soulsby (1985) found the model to be rather insensitive to changes in the values of c, α, and κ.

138. The model was used to simulate oscillatory boundary layer flow with water depth of 10 m; bed roughness of 0.5 cm; steady surface current speed of 1 m/sec; 8-sec waves with incident angles of 0, 45, and 90 deg; and near-bottom velocity amplitudes of 0.5, 1.0, and 1.5 m/sec. Distributions of velocity, turbulent energy, eddy viscosity, and shear stress for wave-current interaction cases were presented. Simulations with a steady current and oblique waves showed that the instantaneous velocity vector varies in a highly nonlinear manner with the amount of turbulent energy acting to retard the near-bottom flow. It was also found that, as a result of the different amounts of turbulent energy generated in the two halves of the wave cycle, the wave cycle averaged horizontal velocity veers away from the direction of wave propagation. Thus, the final angle between the current and waves is greater than the initial oblique angle. The degree of veering varied significantly over the water depth. For example, in one simulation with an initial incident wave angle of 45 deg, the veering angle of the mean velocity vector varied from 15 deg near the bottom to 4 deg at the water surface. The depth-averaged current veered 4.6 deg, which would definitely affect sediment transport calculations under wave-current combined flows. The model also simulated the nonlinear amplification of the bed shear stress and the increase in the oscillatory wave-current boundary layer thickness resulting from wave-current interaction. Details of the case studies are given by Davies, Soulsby, and King (1988).

Stratification effects

139. The degree to which salinity and suspended sediment stratification affect the wave- and current-induced flow, as well as the ability of the flow to stratify, are strongly coupled to wave motion (Grant and Madsen 1986). For example, the relatively large bed shear stresses generated by wave-induced

oscillatory motion often result in resuspension of large quantities of sediment, which may cause the flow to stratify. Nevertheless, Glenn and Grant (1987) found that sediment stratification does not occur within the wave boundary layer for typical continental shelf conditions due to small concentration gradients usually present. However, suspended sediment gradients under estuarine flow conditions may be one to two orders of magnitude greater than those that occur on the shelf, and thus can greatly affect the wave- and current-induced boundary layer flow. Efforts at modeling the effects of salinity and suspended sediment stratification on bed shear and boundary layer flows in combined waves and currents are reviewed here.

140. Hagatun and Eidsvik (1986) describe a turbulence closure model that simulates sediment stratified oscillatory turbulent boundary layer flows. The following assumptions are incorporated in their model: negligible interaction effects between suspended sediment particles, except for the fall velocity component; suspended particles advected at the local flow velocity; collinear waves and currents; settling velocity of sediment particles set equal to a constant; horizontal scale of the mean flow assumed to be much greater than the thickness of the wave-current boundary layer, so that horizontal convective acceleration and mean vertical velocity terms can be neglected in the momentum equations. The equations for momentum and mass conservation then reduce to

$$\frac{\partial \bar{\rho}\bar{u}}{\partial t} = -\frac{\partial \bar{p}}{\partial x} + \frac{\partial}{\partial y}\left[\bar{\rho}(\nu_t + \nu_L)\frac{\partial \bar{u}}{\partial y}\right] \tag{130}$$

$$\frac{\partial \bar{c}}{\partial t} = \frac{\partial}{\partial y}\left[\bar{c}W_s + \left(\frac{\nu_t}{\sigma_t} + \nu_L\right)\frac{\partial \bar{c}}{\partial y}\right] \tag{131}$$

where

$\bar{\rho}$ = mass averaged density

$\bar{u}$ = mass averaged velocity

ν_L = molecular viscosity

c = sediment volume concentration

W_s = fall velocity

σ_t = Prandtl-Schmidt number

Turbulent viscosity is related to turbulent kinetic energy K and turbulence dissipation ϵ by

$$\nu_t = C_\mu K^2 \epsilon^{-1} \tag{132}$$

where C_μ is a constant. The system of equations is closed by the following equations for K and ϵ :

$$\frac{\partial K}{\partial t} = \frac{\partial}{\partial y}\left[\left(\frac{\nu_t}{\sigma} + \nu_L\right)\frac{\partial K}{\partial y}\right] + M + G - \epsilon \tag{133}$$

$$\frac{\partial \epsilon}{\partial t} = \frac{\partial}{\partial y}\left[\left(\frac{\nu_t}{\sigma_\epsilon} + \nu_L\right)\frac{\partial \epsilon}{\partial y}\right] + [C_1(M + G) - C_2\epsilon]\frac{\epsilon}{K} \tag{134}$$

where the indexed values of C and σ are experimental coefficients, M is mechanical energy production, and G is buoyant energy production. The latter two terms are equal to

$$M = \nu_t \left(\frac{\partial \bar{u}}{\partial y}\right)^2 \qquad G = g\,\frac{\Delta\rho}{\rho}\left(\frac{\nu_t}{\sigma_c}\right)\frac{\partial \bar{c}}{\partial y} \tag{135}$$

141. Equations 130-135 are solved using an implicit finite difference scheme using a time-step of $T/120$ where T is the wave period. Comparisons to existing data sets were made for predicted phase variations of sediment concentration, height variation of period averaged sediment concentration, maximum horizontal sediment flux, and mean velocity and shear stress profiles. Good to excellent agreements between the measured and predicted quantities were achieved in all cases. As Hagatun and Eidsvik point out, the main weakness of their modeling approach is associated with simulating bed interaction.

142. Glenn and Grant (1987) describe an eddy diffusivity closure model that accounts for suspended sediment stratification. The model is an extension of the wave and current models developed by Grant and Madsen (1979) for a

fixed bed and by Grant and Madsen (1982) for movable beds. The eddy diffusivity closure scheme is used to couple the unsteady momentum and sediment mass conservation equations, which are solved for the combined wave and current boundary layer flow, sediment mass distribution, and suspended sediment transport rate. The model also accounts for ripple formation and degradation, near-bed sediment transport, and suspended sediment induced stratification. The latter process is represented in the closure scheme by applying a stratification correction to the neutral, time-invariant eddy viscosity. The stratification correction term was found to be negligible within the wave boundary layer. Thus, sediment stratification is simulated to occur outside the wave boundary layer only. The neutral eddy viscosity is taken to be proportional to the wave-current shear velocity and varies linearly with height above the bed.

143. Since the model represents movable bed effects, and therefore is not within the scope of this report, only some of the results/conclusions from this modeling effort are discussed. However, it appears that at the present time, this model by Glenn and Grant is the most promising in terms of representing the pertinent flow and sediment processes in estuarine boundary layer flows. Nevertheless, the model is limited to consideration of cohesionless sediment transport, and thus is not capable of simulating cohesive sediment transport and related phenomena (e.g., fluid mud formation/movement, bed consolidation).

144. Model simulations showed that the current velocity-induced shear and the vertical decay rate of suspended sediment concentration are diminished within the wave boundary layer. This increased energy dissipation in the wave boundary layer also causes the current outside the wave layer to experience an effective (or apparent) bottom roughness that is larger than the actual bed roughness. Above the wave boundary layer, the current-induced shear and sediment concentration decay rate are increased, even more so by suspended sediment stratification.

PART V: CONCLUSIONS AND RECOMMENDATIONS

145. These conclusions and recommendations are interim in that (a) they represent a set of qualitative opinions based on the authors' review of literature, personal experience, and judgment; and (b) experimental work is ongoing to test the validity of the conclusions reached here so that a final set of conclusions can be formulated in a later report.

Conclusions

Estuarine flow

146. Conventional steady-flow equations (Equations 9-13) for boundary layer velocity profiles and bed stresses can be seriously misleading when applied to sediment transport problems in estuarine flows. They have been used with considerable success in providing estimates of water levels and general flow patterns in manual calculations and two-dimensional depth-integrated numerical models. They have even been used in sediment transport calculations, but their use requires considerable skill and knowledge. Better descriptions are needed for detailed (high temporal and spatial resolution) analysis of dredged material placed in open water.

147. The following conclusions are drawn from this review:

a. For cases where limited resources prevent the most rigorous boundary layer descriptions, Equations 18-28 may be sufficient for rapid estimates of sediment transport.

b. When using Equations 18-28, to take into account salinity-induced stratification in computation of bed shear (or u_*) and velocity profiles in estuarine flows, the method developed by McCutcheon (Equation 35) is recommended. For suspended sediment stratified flows, it is recommended that the values for bed shear obtained using the method presented by Coleman (Equation 38) be compared to those obtained using McCutcheon's method. Both methods require iterative solution of the governing equations for vertically nonuniform density profiles. However, Gust's findings, paragraphs 74-80, regarding occurrence of drag reduction in sediment suspensions (which causes alterations in the velocity profile, in particular in the near-bed zone) should be kept in mind.

c. For three-dimensional modeling and highly detailed sediment transport calculations, turbulence transport modeling by Mellor-Yamada (Equation 37) is most appropriate and, depending on resources, is recommended.

Estuarine flows with short-period waves

148. The following methods are recommended for computation of bed shear stresses in estuarine flows with short-period waves:

a. O'Connor and Yoo's method (Equations 65-75) is recommended when complete numerical modeling of the water column is not practical/possible.

b. Of the eddy viscosity models reviewed, and considering the limited scope of analysis in this report, i.e., fixed bed, Madsen and Wikramanayake's model (Equations 100-104 and 113-115) is recommended.

c. The turbulence model proposed by Davies, Soulsby, and King, paragraphs 128-137, is recommended over other turbulence closure models when sediment stratification does not occur because of its realistic approach in defining the problem, and because of its relative simplistic approach compared with other turbulence closure schemes.

d. When stratification does occur, the turbulence closure model described by Glenn and Grant (1987) is recommended.

Recommendations

149. Field and laboratory data should be used to define the circumstances under which these conclusions given are sound. Numerical experiments using laboratory and field data as guides should be used to establish the computational resources required for the various levels of turbulence closure complexity.

150. After the appropriate expressions for boundary layer descriptions over firm beds have been selected, they should be adapted for soft/flowable beds using the general approach of Mei and Liu (1987).

REFERENCES

Abbott, M. R. 1960. "Salinity Effects in Estuaries," Journal of Marine Research, Vol 18, No. 2.

Bijker, E. W. 1966. "The Increase of Bed Shear in a Current Due to Wave Motion, "Proceedings, 10th Conference on Coastal Engineering, American Society of Civil Engineers, New York.

Blumberg, A. F., and Kantha, L. H. 1986. "Computing Storm-Induced Currents Using Second Moment Turbulence Closure" (in preparation), Draft chapter for American Society of Civil Engineers publication, "Physics-Based Environmental Modeling of Estuaries."

Bowden, K. F., Fairbairn, L. A., and Hughes, P. 1959. "The Distribution of Shearing Stresses in a Tidal Current," Geophysical Journal of the Royal Astronomical Society, Vol 2.

Bradshaw, P., Cebeci, T., and Whitelaw, J. H. 1981. Engineering Calculation Methods for Turbulence, Academic Press. New York.

Brevik, I., and Aas, B. 1980. "Flume Experiment on Waves and Currents; I: Rippled Bed," Coastal Engineering, Vol 3.

Cheng, R. T., Wang, J., and Gartner, S. W. 1988. "Graviational Circulation in Well Mixed and Partially Mixed Estuaries," Proceedings, Conference, Physics of Shallow Bays and Estuaries, Nov 1988, Asilomar, CA, Springer-Verlag, Berlin.

Coleman, N. L. 1981. "Velocity Profiles with Suspended Sediment," Journal of Hydraulic Research, Vol 19, No. 3.

Coles, D. 1956. "The Law of the Wake in the Turbulent Boundary Layer," Journal of Fluid Mechanics, Vol 14.

Collins, J. I. 1964. "Effect of Currents on Mass Transport of Progressive Water Waves," Journal of Geophysical Research, Vol 69, No. 6.

Davies, A. G., Soulsby, R. L., and King, H. L. 1988. "A Numerical Model of the Combined Wave and Current Bottom Boundary Layer," Journal of Geophysical Research, Vol 93, No. C1.

Donnelly, R. J. 1988 (Nov). "Superfluid Turbulence," Scientific American.

Einstein, H. A., and Abdel-Aal, F. M. 1972. "Einstein Bed-Load Function at High Sediment Rates," Journal of the Hydraulics Division, American Society of Civil Engineers, Vol 98, No. HY1.

Einstein, H. A., and Chien, N. 1954. "Second Approximation to the Solution of the Suspended Load Theory," Institute of Engineering Research, University of California, Berkeley, CA.

_____. 1955. "Effects of Heavy Sediment Concentration Near the Bed on Velocity and Sediment Distribution," Institute of Engineering Research, University of California, Berkeley, CA.

Fortier, J. R., and Scobey, F. C. 1926. "Permissible Canal Velocities," Transactions, American Society of Civil Engineers, Vol 89.

French, R. H. 1977. "Modification of the Chezy Roughness Coefficient by Density Stratification," Hydraulics in the Coastal Zone, Proceedings, 25th Annual Hydraulics Division Specialty Conference, 10-12 August 1977, Texas A&M University, College Station, TX, American Society of Civil Engineers, New York.

George, C. B., and Sleath, J. F. A. 1979. "Measurements of Combined Oscillatory and Steady Flow over a Rough Bed," Journal of Hydraulic Research, Vol 17, No. 4.

Glenn, S. M., and Grant, W. D. 1987. "A Suspended Sediment Stratification Correction for Combined Wave and Current Flows," Journal of Geophysical Research, Vol 92, No. C8.

Gordon, C. M. 1975. "Sediment Entrainment and Suspension in a Turbulent Tidal Flow," Marine Geology, Vol 18.

Grant, W. D., and Madsen, O. S. 1979. "Combined Wave and Current Interaction with a Rough Bottom," Journal of Geophysical Research, Vol 84, No. C4.

_____. 1982. "Moveable Bed Roughness in Unsteady Oscillatory Flow," Journal of Geophysical Research, Vol 87.

_____ _____. 1986. "The Continental-Shelf Bottom Boundary Layer," Annual Review of Fluid Mechanics, Vol 18.

Gust, G. 1976. "Observation of Turbulent-drag Reduction in a Dilute Suspension of Clay in Sea-water," Journal of Fluid Mechanics, Vol 75, Part 1.

Gust, G., and Southard, J. B. 1983. "Effects of Weak Bed Load on the Universal Law of the Wall," Journal of Geophysical Research, Vol 88, No. C10.

Gust, G., and Walger, E. 1976. "The Influence of Suspended Cohesive Sediments on Boundary-Layer Structure and Erosive Activity of Turbulent Seawater Flow," Marine Geology, Vol 22.

Hagatun, K., and Eidsvik, K. J. 1986. "Oscillating Turbulent Boundary Layer With Suspended Sediments," Journal of Geophysical Research, Vol 91, No. C11.

Halliwell, A. R., and O'Connor, B. A. 1968. "Shear Velocity in a Tidal Estuary," Proceedings, 11th Conference on Coastal Engineering, American Society of Civil Engineers, New York.

Hino, M. 1963. "Turbulent Flow with Suspended Particles," Journal of the Hydraulics Division, American Society of Civil Engineers, Vol 89, No. HY4.

Hinze, J. O. 1959. Turbulence, McGraw-Hill, New York.

Ippen, A. T. 1971. "A New Look at Sedimentation in Turbulent Streams," Journal of the Boston Society of Civil Engineers, Vol 58, No. 3.

Jonsson, I. G. 1965. "Friction Factor Diagrams for Oscillatory Boundary Layers," Basic Research Progress Report No. 10, Technical University of Denmark, Copenhagen.

_____. 1966. "The Friction Factor for a Current Superimposed by Waves," Basic Research Progress Report No. 11., Technical University of Denmark, Copenhagen.

Kajiura, K. 1968. "A Model of the Bottom Boundary Layer in Water Waves," Bulletin No. 46, Earthquake Research Institute, University of Tokyo, Tokyo, Japan.

Kamphuis, J. W. 1975. "Friction Factor Under Oscillatory Waves," Journal of the Waterways, Harbors, and Coastal Engineering Division, American Society of Civil Engineers, Vol 101, WW2.

King, H. L., Davies, A. G., and Soulsby, R. L. 1985. "A Numerical Model of the Turbulent Boundary Layer Beneath Surface Waves and Tides," I.O.S. Report No. 196, Institute for Oceanographic Sciences, Tauton, England.

King, I. P. 1988. "A Model for Three-Dimensional Density Stratified Flow," RMA 8523, Resource Management Associates, Lafayette, CA.

Knight, D. W. 1978. "Review of Oscillatory Boundary Layer Flow," Journal of the Hydraulics Division, American Society of Civil Engineers, Vol 104, No. HY6.

Lavelle, J. W., and Mofjeld, H. O. 1983. "Effects of Time-Varying Viscosity on Oscillatory Turbulent Channel Flow," Journal of Geophysical Research, Vol 88, No. C12.

Lesht, B. M. 1978. "Field Measurements of the Bottom Frictional Boundary Layer in the New York Bight," Technical Memorandum ERL MESA-28, Marine Ecosystems Analysis Program, National Oceanic and Atomspheric Administration, Boulder, CO.

Ludwick, J. C. 1973. "Tidal Currents and Zig-Zag Sand Shoals in a Wide Estuary Entrance," TR No. 7, Institute of Oceanography, Old Dominion University, Norfolk, VA.

Lyles, L., and Woodruff, N. P. 1972. "Boundary Layer Flow Structure: Effects on Detachment of Noncohesive Particles," Sedimentation, H. W. Shen, ed., Fort Collins, CO.

Madsen, O. S., and Wikramanayake, P. N. 1988. "Simple Models for Turbulent Wave-Current Bottom Boundary Layer Flow," Contract Report DRP-91-1, Prepared by Ralph M. Parsons Laboratory, Massachusetts Institute of Technology, Cambridge, MA, for US Army Engineer Waterways Experiment Station, Vicksburg, MS.

Markatos, N. C. 1986. "The Mathematical Modelling of Turbulent Flows," Appli. Math Modeling, Vol. 10, June.

McAnally, W. H., Letter, J. V., and Thomas, W. A. 1986. "Two- and Three-Dimensional Modeling Systems for Sedimentation," River Sedimentation, Proceedings, Hydraulics Division Specialty Conference, Jackson, MS, American Society of Civil Engineers, New York.

McCutcheon, S. C. 1981. "Vertical Velocity Profiles in Stratified Flows," Journal of the Hydraulics Division, American Society of Civil Engineers, Vol 107, No. 3.

Mehta, A. J., and Christensen, B. A. 1977. "Incipient Sediment Motion in Entrances with Shell Beds," Coastal Sediments '77, Proceedings, Conference, American Society of Civil Engineers, New York.

Mei, C. C., and Liu, K. F. 1987. "A Bingham-Plastic Model for A Muddy Seabed Under Long Waves," Journal of Geophysical Research, Vol 92, No. C13.

Mellor, G. L., and Gibson, D. M. 1966. "Equilibrium Turbulent Boundary Layers," Journal of Fluid Mechanics, Vol 24.

Mellor, G. L., and Yamada, T. 1982. "Development of a Turbulence Closure Model for Geophysical Fluid Problems," Reviews of Geophysics and Space Physics, Vol 20, No. 4.

Monin, A. S., and Yaglom, A. M. 1971. "Statistical Fluid Mechanics" ("Statisicheskaya Gidromekhanika—Mekhhanika Turbulentnosti"), MIT Press, Cambridge, MA.

O'Connor, B. A., and Yoo, D. 1988. "Mean Bed Friction of Combined Wave/ Current Flow," Coastal Engineering, Vol. 12.

Ordonez-C., N. A. 1970. "The Absolute Concentration Distribution of Suspended Sediment in Turbulent Streams," Ph.D. dissertation, Massachusetts Institute of Technology, Boston, MA.

Richards, D. R., and Bach, D. P. 1988. "A Numerical Model Analysis of Mississippi River Passes Navigation Channel Improvements, Three-Dimensional Numerical Model Results," Report 5, Miscellaneous Paper HL-87-2, US Army Engineer Waterways Experiment Station, Vicksburg, MS.

Rodi, W. 1982. "The Modelling of Turbulent Flows Using Transport Equation Models," Proceedings, Symposium-IAHR: Refined Modeling of Flows, Presses de l'Ecole Natl des Ponts et Chaussees, Paris.

_____. 1987 (May 15). "Examples of Calculation Methods for Flow and Mixing in Stratified Fluids," Journal of Geophysical Research, Vol 92, No C5.

Schlicting, H. 1968. Boundary-Layer Theory, J. Kestin, translator, 6th ed., McGraw-Hill, New York.

Scottron, V. E. 1967. "Turbulent Boundary Layer Characteristics Over a Rough Surface in an Adverse Pressure Gradient," Report No. 2659, Naval Ship Research and Development Center. Alexandria, VA.

Sleath, J. F. A. 1984. Sea Bed Mechanics, Wiley, New York.

Smith, J. D., and McLean, S. R. 1977. "Spatially Averaged Flow over a Wavy Surface," Journal of Geophysical Research, Vol 82, No. 12.

Soulsby, R. L. 1983. "The Bottom Boundary Layer of Shelf Seas," Physical Oceanography of Coastal and Shelf Seas, B. Johns, ed., Elsevier, Amsterdam, The Netherlands, Chapter 5.

Soulsby, R. L., and Dyer, K. R. 1981. "The Form of the Near-Bed Velocity Profile in a Tidally Accelerating Flow," Journal of Geophysical Research, Vol 86, No. C9.

Sternberg, R. W. 1968. "Friction Factors in Tidal Channels with Differing Bed Roughness," Marine Geology, Vol 6, No. 3.

Swart, D. H. 1974. "Offshore Sediment Transport and Equilibrium Beach Profiles," Delft Publication No. 131, Delft Hydraulics Laboratory, The Netherlands.

Takemitsu, N. 1988. "Revised k-e Model (A Turbulence Model)," Computational Methods in Flow Analysis, Proceedings, International Conference on Computational Method in Flow, Okayama University of Science, 5-8 September 1988, Okayama, Japan.

Tanaka, H., and Shuto, N. 1981. "Friction Coefficient for a Wave-Current Coexistent System," Coastal Engineering in Japan, Vol 24.

Tanaka, H., Chian, C. S., and Shuto, N. 1983. "Experiments on an Oscillatory Flow Accompanied with a Unidirectional Motion," Coastal Engineering in Japan, Vol 26.

Task Committee on Turbulence Models in Hydraulic Computations. 1988. "Turbulence Modeling of Surface Water Flow and Transport: Parts I-V," Journal of Hydraulic Engineering, American Society of Civil Engineers, Vol 114, No. HY9.

Tesche, T. W. 1975. "Temporal Estuarine Shear Stress Distributions," National Convention, American Society of Civil Engineers, Denver, CO.

Thomas, William A., and McAnally, William H., Jr. 1985 (Jul). "User's Manual for the Generalized Computer Program System: Open-Channel Flow and Sedimentation, TABS-2," Instruction Report HL-85-1, US Army Engineer Waterways Experiment Station, Vicksburg, MS.

Vager, B. G., and Kagan, B. A. 1969. "The Dynamics of the Turbulent Boundary Layer in a Tidal Current," Izvestiya Academy Sciences, USSR Atmospheric and Oceanic Physics, English Translation, Vol 5, No. 2.

Vanoni, V. A. 1946. "Transportation of Suspended Sediment by Water," Transactions of the American Society of Civil Engineers, Vol III.

Wang, S. 1981. "Variation of Karman Constant in Sediment-Laden Flow," Journal of the Hydraulics Division, American Society of Civil Engineers, Vol 107, No. HY4.

Table 1

Friction Factor Experssion from Theoretical Velocity Profiles

Law	Expression	Applicable Zone	Flow/Boundary Restriction
Modified von Karman-Prandtl	$f_c = 2\left[\frac{1}{\kappa} \ln\left(\frac{y}{k_s} + 0.00338\right) + 8.5\right]^{-2}$	$y < 0.15\delta$	$\frac{u_* k_s}{\nu} \geq 74$
Velocity defect	$f_c = 2\frac{1 - 2\frac{u}{U_o} + \frac{u^2}{U_o^2}}{\left(3.7 \ln \frac{\delta}{y}\right)^2}$	$1 \geq y \geq 0.15$	none
Power law	$f_c = 2\left(\frac{8.74^7 uy}{\nu}\right)^{-1/4}$	$y \leq \delta$	$70{,}000 > \frac{u_*}{\nu} > 30{,}000$

Note: δ = boundary layer thickness
U_o = free-stream velocity

Table 2

Roughness Coefficient Estimates

Source	Conditions	f_c
Bowden, Fairbairn, and Hughes (1959)	u at 5 percent	0.007
Sternberg (1968)	u at 100 cm	0.006
Tesche (1975)	u at 50 cm	0.007
Equation 10	n = 0.02 , R = 30 ft	0.004
Equation 10	k_s = 0.2 mm , R = 30 ft	0.0004
Equation 11	k_s = 0.2 mm , y = 3 ft	0.0023
Equation 12	u = 3 fps , y = 3 ft	0.0016
Soulsby (1983)	Mud bottom, u at 100 cm	0.0011
	Silt and sand bottom, u at 100 cm	0.0008
	Plane sand, u at 100 cm	0.0013
	Rippled sand, u at 100 cm	0.0030
	Sand and gravel, u at 100 cm	0.0012

APPENDIX A: NOTATION

Parts II and III

A	Integration constant
b	Channel width
c	Sediment volume concentration
c_o	Maximum (near-bed) sediment volume concentration
c_m	Depth-averaged sediment volume concentration
C	Chezy friction coefficient
e	Alternating tensor
E_D	Fickian diffusion coefficient
f	Darcy friction factor
f_c	Current friction factor = $f/4$
g	Acceleration of gravity
G	Buoyancy contribution to turbulent energy
h	Mean water depth
i,j,k	Coordinate axis designator, 1, 2, or 3 with repeated index summation
k	Turbulent kinetic energy
k_s	Effective roughness size
ℓ	Mixing length
n	Manning roughness coefficient; index for multiple constituents in transport; subscript indicating constituent
P_s	Shear production of turbulent energy
P	Pressure
r	Ratio of mass mixing length to momentum mixing length
R	Hydraulic radius
R_f	Flux Richardson number
R_i	Richardson number

S	Sediment specific gravity
t	Time
T	Period of oscillation
u	Flow velocity in direction of x axis
u_1	Velocity at specified distance above the bed
$\bar{u}$	Depth-averaged flow velocity
u_*	Shear velocity = $\sqrt{\tau/\rho}$
u_{*cw}	Wave- and current-induced shear velocity
U_o	Free-stream velocity
W_s	Sediment settling velocity
x	Horizontal distance coordinate
y	Vertical distance coordinate
y_o	Bed roughness height
z	Horizontal distance coordinate perpendicular to x
δ	Boundary layer thickness
δ_o	Thickness of all three layers in Kajiura's three-layer model
δ_1	Inner layer thickness
ϵ	Dissipation of turbulence
η	Displacement of the water surface from mean water level
Θ	Concentration of constituent
κ	Von Karman's turbulence constant
Λ_1	Length scale
ν	Kinematic viscosity of water
ν'	Kinematic viscosity of solid-liquid mixture
ν_t	Turbulent eddy viscosity
ν_{tR}	Reference value of eddy viscosity
Π	Wake strength coefficient

$(\Pi/\kappa)\omega(y/\delta)$	Wake region velocity augmentation function
ρ	Density of water
ρ_b	Density of sediment-water mixture at the sediment bed
ρ_h	Density of sediment-water mixture at the water surface
ρ_m	Depth-averaged density of sediment-water mixture
ρ_s	Sediment density
ρ_o	Reference density
σ	Frequency of oscillation
σ_t	Turbulent Prandtl number
τ	Bed shear stress
τ_{sw}	Sidewall shear stress
ϕ	Sum of sinks and source for θ
Ω	Coriolis effect parameter

Superscripts

'	A quantity fluctuating in time

Subscripts to τ and δ

xy	In the x direction on a y constant surface
xz	In the x direction on a z constant surface
^	Instantaneous value

Part IV

a	Amplitude of water-surface motion
A_o	Wave orbit horizontal amplitude
A_{ob}	Wave orbit horizontal amplitude at the bed
c	Sediment volume concentration
C	Chezy friction coefficient
d	Height of inner layer of two-layer viscosity model
f_c	Current friction factor = $f/4$
f_w	Wave friction factor
f_{wc}	Friction factor for combined waves and currents
g	Acceleration of gravity
G	Buoyant turbulent energy production
h	Depth of flow
k	Wave number = $2\pi/L$
k_b	Characteristic dimension of bottom roughness
k_n	Boundary roughness size
k_s	Equivalent bed roughness size
K	Turbulent kinetic energy
L	Wave length
ℓ	Mixing length
ℓ'	Measure of wave boundary layer thickness
M	Mechanical energy production
p	Pressure
∇p	Mean pressure gradient
t	Time
T	Period of oscillation

T_{yz} Reynolds shear stress in the z-direction associated with the current

u Velocity in direction of x axis

$\bar{u}$ Mass averaged velocity

u_1 Velocity in x-direction at specified distance above the bed

$u_b^*(t)$ Magnitude of modified shear velocity

u_{bm} Maximum wave velocity at the top of the wave boundary layer

u_d Wave-induced orbital velocity within wave boundary layer

u_o Wave orbital horizontal velocity

u_{om} Maximum wave orbital velocity near the bed

u_r Resultant velocity of simultaneous wave and flow

u_* Shear velocity = $\sqrt{\tau/\rho}$

u_b Near bottom velocity

$\widehat{u_{*c}}$ Shear velocity associated with the current boundary shear stress

$|u_{*c}|$ Magnitude of the time-averaged shear velocity

$|u_{*wc}|$ Magnitude of maximum shear velocity due to combined wave and current motion

U_∞ Amplitude of the horizontal wave-induced velocity component immediately above the wave boundary layer

U Depth-averaged current speed

$|U_a|$ Magnitude of steady current velocity at height y = a above the bottom

U_o Free-stream velocity

$\bar{U}$ Laminar current velocity at $y = 5/(\sigma/2\nu)^{0.5}$

v Velocity in direction of y axis

w Velocity in direction of z axis

W_s Sediment settling velocity

x Horizontal distance coordinate

y Vertical distance coordinate

y' Hypothetical elevation above the bed (proposed by Bijker) where a line emanating from the seabed ($y = h$) is tangential to the current-only velocity profile

y_1 Height above the theoretical bed at which the velocity is equal to zero

y_o Bed roughness height

z Horizontal distance coordinate

α Current velocity reduction factor

α' Ratio of eddy diffusivities of turbulent energy and momentum

δ Boundary layer thickness

δ_w Wave boundary layer thickness

ϵ Turbulence dissipation rate

η Displacement of the water surface from mean water level

Θ Angle between orbital wave motion and the direction normal to the current

κ Von Karman's turbulence constant

μ Relative velocity of maximum wave orbital velocity to the current at y'

ν Kinematic viscosity of water

ν_L Molecular viscosity

ν_t Turbulent eddy viscosity

ρ Density of water

$\bar{\rho}$ Mass averaged density

σ Wave angular frequency

σ_c Turbulent Prandtl number

τ Bed shear stress

τ_b Bed shear

τ_{bm} Maximum wave- and current-induced bed shear

τ_c Bed shear stress due to current only

τ_m Maximum combined wave-current bed shear stress vector

τ_w Maximum wave bottom shear stress

τ_{wc} Resultant combined shear due to waves and currents

$\bar{\tau}_b$ Current-induced time mean bed shear stress

$\bar{\tau}_{wc}$ Time mean wave and current induced bed shear stress

ϕ Angle between current and wave motion directions

$\bar{\phi}_c$ Angle of the average shear stress

Superscripts to τ and δ

' Surface (grain or net) shear

" Form shear

No superscript indicates total shear

Subscripts to τ and δ

c Caused by current

w Caused by waves

wc Caused by waves plus currents

xy In the x direction on a y constant surface

xyo In the x direction at the bed (y = 0)

xz In the x direction on a z constant surface

Waterways Experiment Station Cataloging-In-Publication Data

McAnally, William H.

Boundary stresses and velocity profiles in estuarine flows. Report 1, Interim calculation methods / by William H. McAnally, Jr., Earl J. Hayter ; prepared for Department of the Army, US Army Corps of Engineers ; monitored by Coastal Engineering Research Center, U.S. Army Engineer Waterways Experiment Station.

92 p. : ill. ; 28 cm. — (Technical report ; DRP-92-3 rept. 1)

Includes bibliographical references.

1. Estuarine oceanography — Mathematics. 2. Boundary layer. 3. Hydrodynamics. 4. Tide-waters. I. Hayter, E. J. II. United States. Army. Corps of Engineers. III. Coastal Engineering Research Center (U.S.) IV. U.S. Army Engineer Waterways Experiment Station. V. Dredging Research Program. VI. Title. VII. Series: Technical report (U.S. Army Engineer Waterways Experiment Station) ; DRP-92-3 rept. 1. TA7 W34 no.DRP-92-3 rept.1